CHALMERS
UNIVERSITY OF TECHNOLOGY

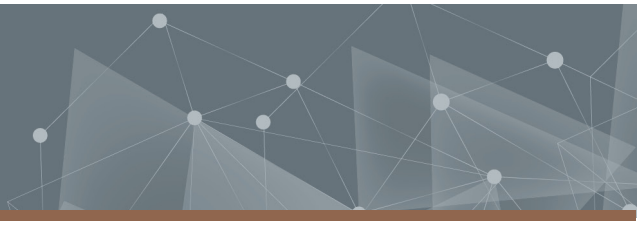

The effect of sample composition on acoustic droplet ejection of small molecules in DMSO

Increasing the efficiency of compound handling in pharmaceutical R&D

Master's thesis in Materials Chemistry

SEBASTIAN LADISIC

DEPARTMENT OF CHEMISTRY AND CHEMICAL ENGINEERING

CHALMERS UNIVERSITY OF TECHNOLOGY
Gothenburg, Sweden 2023
www.chalmers.se

Master's thesis 2023

The effect of sample composition on acoustic droplet ejection of small molecules in DMSO

Increasing the efficiency of compound handling in pharmaceutical R&D

SEBASTIAN LADISIC

CHALMERS
UNIVERSITY OF TECHNOLOGY

Department of Chemistry and Chemical Engineering
Division of Applied Chemistry
Chalmers University of Technology
Gothenburg, Sweden 2023

The effect of sample composition on acoustic droplet ejection of small molecules in DMSO. Increasing the efficiency of compound handling in pharmaceutical R&D
SEBASTIAN LADISIC

Supervisor: Martin Svensson, AstraZeneca
Examiner: Anette Larsson, Department of Chemistry and Chemical Engineering

Master's Thesis 2023
Department of Chemistry and Chemical Engineering
Division of Applied Chemistry
Chalmers University of Technology
SE-412 96 Gothenburg
Telephone +46 31 772 1000

The effect of sample composition on acoustic droplet ejection of small molecules in DMSO. Increasing the efficiency of compound handling in pharmaceutical R&D
SEBASTIAN LADISIC
Department of Chemistry and Chemical Engineering
Chalmers University of Technology

Abstract

AstraZeneca is pioneering within life science research and development, and contributes significantly in reducing the numbers of deaths caused by non-communicable diseases. Laboratory automation has contributed to the heavily increased number of screening assays in modern times and AstraZeneca has teamed up with Brooks Life Sciences, Beckman Coulter Life Sciences and Titian, to create a workflow that uses acoustic droplet ejection for transferring low volumes of liquid samples in an efficient and risk free process. Samples that pose problems in the liquid handler are removed from the chemical library and thus slow down the drug discovery and development process. This study evaluates any correlation between failure in acoustic dispensing and the sample composition of 50 suspensions of different small molecules in dimethyl sulfoxide. The samples are characterized by their solid particle shape, size and crystallinity, and a liquid chromatography - mass spectrometry method is developed to determine if the precipitate represents the original compound. Five sizes of poly(methyl metacrylate) microspheres are used in model suspensions for evaluating the interaction between solid particles and the acoustic signals. The results show that no suspension is contaminated and that the acoustic dispensing is not dependent on size, shape or crystallinity of the precipitate particles. The dispensing failure probably occurs from a combination of reflection and scattering of the acoustic signal that measures the sample volume in the tubes, and seems to be dependent on the amount of solid particles and their position on the tube bottom. This study concludes that the bare presence of solid particles is enough to make a sample incompatible with acoustic dispensing, and a reasonable solution is to implement a separate workflow for compounds that are poorly soluble in the solvent of choice. An alternative workflow is presented in the final section of the report.

Keywords: Acoustic dispensing, Sample characterization, Solubility, Liquid chromatography, Mass Spectrometry

Acknowledgements

I would like to thank the Compound Synthesis and Management department of AstraZeneca for trusting me with the assignment to perform this study. A special thank you to the group in Mölndal for the warm welcome and for always making me feel as a part of the team. I would also like to pay a special thank you to my supervisor Martin Svensson for helping me to push the project in the correct direction, and always getting me in touch with the right people when we needed help or clarification. Thank you Karin Kaspersson for additional support in my project and for always making sure I stayed on track. Thank you Silvio di Castro for always being available to answer questions and to discuss solutions, and for always being happy to discuss the italian culture during the coffee breaks. I would also like to thank my examiner prof. Anette Larsson for accepting me as a thesis worker and for helping me with valuable insights throughout the project, and for always caring about how I am feeling with the project.

Thank you Lennart Lindfors, Thierry Kogej, Lisa Wissler and Chichi Qi at AstraZeneca for contributing with your competence and helping me start in the right direction. Thank you Carl Jarman, Laleta Mahey and Kseniya Korchagina from Beckman Coulter Life Sciences for answering my questions and for helping me in the laboratory.

A very special thank you to the members of AZ inspire for many entertaining lunch- and coffee breaks, and for being fantastic friends both on and off work.

Sebastian Ladisic, Gothenburg, June 2023

List of Acronyms

Below is the list of acronyms that have been used throughout this thesis listed in alphabetical order:

ADE	Acoustic Droplet Ejection
CM	Compound Management
DFA	Dynamic Fluid Analysis
DMSO	Dimethyl Sulfoxide
EAT	Electro Acoustic Transducer
ESI	Electrospray Ionization
FFT	Fast Fourier Transform
HTS	High Throughput Screening
LC	Liquid Chromatography
MS	Mass Spectrometry
NCD	Non-Communicable Disease
NP	Normal Phase
PMMA	Poly(Methyl Metacrylate)
RF	Radio Frequency
RP	Reverse Phase
TOF	Time Of Flight
UV-Vis	Ultraviolet and Visible
WHO	World Health Organization

Nomenclature

Below is the nomenclature of variables that have been used throughout this thesis.

Variables

Solubility thermodynamics

ΔG	Gibb's free energy of dissolution
ΔH	Enthalpy of dissolution
ΔH_l	Lattice enthalpy
ΔH_{hyd}	Enthalpy of hydration
T	Temperature
ΔS	Entropy of dissolution

Wave physics

T	Period
λ	Wavelength
f	Frequency
v	Sound velocity
κ	Adiabatic compressibility
ρ	Density
A_i	Amplitude of incident wave
A_r	Amplitude of reflected wave
Z	Acoustic impedance
R	Reflection coefficient
l	Length of boundary or bounded object that interferes sound wave
r	Radius of sphere

ka	Factor determining importance of scattering and reflection of sound waves interfered by spherical object

Acoustic liquid handling

F	Focal length of lens
$F\#$	F-number
D	Aperture diameter
d	Droplet diameter
d_a	Focal spot size
h	Fluid height
t	Time for reflected sound wave to reach detector
E_{DFA}	Toneburst energy from any DFA measurement
$E_{threshold}$	Threshold toneburst
A	Compound specific constant
B	Compound specific constant

Absorption spectroscopy

A	Absorbance
I_0	Intensity of emitted light
I	Intensity of light after passing through sample
ϵ	Molar absorptivity
l	Length of light path through sample
c	Concentration

Contents

List of Figures

List of Tables

1

Introduction

Each year non-communicable diseases (NCDs), such as cardiovascular diseases, chronic respiratory diseases, diabetes and cancer are responsible for 74 % of all deaths globally [1]. This corresponds to 41 million deaths in all age groups over all geographical locations. There is a significant difficulty in controlling and treating NCDs as they do not spread by infections, but are rather the result from a combination of genetic, physiological, environmental and behavioural factors. The consequences of NCDs are severe enough to be included in the United Nations third goal for sustainable development which states that healthy lives and well being should be ensured and promoted by, amongst others, reducing the death by NCDs with 1/3 by 2030 [2]. A promising decrease has been observed between 2010 and 2019, but the decline rate is still too low to meet the goal. Both the United Nations and WHO suggest that increased detection, screening and treatment of NCDs is the key for making treatment available and affordable to everyone [1] [2].

The future relies on the pharmaceutical industry to follow the recommendations of the United Nations and WHO, to keep reducing the severe health issues related to NCDs. With over 50 years of experience, AstraZeneca is already pioneering within respiratory care, immunology, cancer treatment and cardiovascular diseases, and works in line with the goals for sustainable development stated by the United Nations [3]. Medicines are already provided for treating multiple respiratory diseases and AstraZeneca is constantly pushing the boundaries of science to increase the life saving potential by new medicines. Lest to forget is also the development of vaccines and antibodies that contribute to providing long lasting immunity for millions of individuals against communicative diseases as well, not least highlighted during the recent COVID-19 pandemic. However, research takes time and the drug discovery and development process is not an exception. The time intensive process requires large amounts of iterations before reaching a final product, and each iteration is dependent on the knowledge gained during the previous test [4].

A single department at AstraZeneca can be responsible for synthesizing thousands of new potential drug molecules each year [4]. These molecules undergo millions of assays yearly in order to determine their full potential. However, there is normally an incompatibility between the output from a chemical synthesis and a biological screening assay which requires additional work. The solution to this problem was started in the early 2000s when the Compound Management group (CM) was founded as a department of its own. Its mission is to process and distribute compounds in alternative formats for specific assays. In the early days of the CM group there were approximately 20 high throughput screening (HTS) campaigns to support. This amount of HTS was represented by a chemical library of more than 1 million stored compounds in the CM chemical library. However, the reality quickly changed for the CM group as the drastic development of automation within the pharmaceutical industry increased both the number of synthesized compounds and the number of HTS campaigns. By 2022 the CM group found themselves expected to support more than 70 HTS campaigns, more than a three-fold increase compared to the original demand. The desire to find new target molecules is constantly increasing and the drug discovery and development process is expected to accelerate even more, and thus the CM group can expect even higher workload and pressure in the future.

Newly synthesized compounds are obtained as solids and are to be processed by the CM group in multiple workflows within the department [4]. In most cases, one fraction of the compound is stored as a solid and one fraction is stored as a solution. Some compounds are soluble in water and can thus be kept and used as aqueous solutions. However, the most widely used solvent within the pharmaceutical industry HTS is dimethyl sulfoxide (DMSO) [5]. It dissolves compounds over a broad range of chemical properties, has low volatility, has low toxicity to tissue culture, is miscible with water and can be considered harmless in bioassays at low concentrations. In other words, DMSO is the solvent of choice for an efficient HTS supporting workflow. When the compounds are dissolved they are available for distribution to any compatible screening assay. In modern times the assays have become compatible with multi-well plates that allow multi-compound analysis in time efficient processes. The CM group delivers assay ready plates constructed from an order template that is requested by a department within the company. This requires a liquid transfer from the solution container to the destination plate. The chemical library consists of solutions stored in racks, and to pick the required racks to acquire all compounds that satisfies one specific order has shown to be the slowest step in the delivery process [4].

It is believed that the process is more time efficient if less racks must be combined to fulfil one order, meaning that each racks must fit a larger number of solution vials. Increasing the number of samples on each rack requires smaller sample containers and thus very low volumes, which in turn requires a low-volume compatible liquid transfer method. This is why AstraZeneca has teamed up with Brooks Life Sciences, Beckman Coulter Life Sciences and Titian, to create a pioneering liquid handling system that utilizes energy from sound waves to transfer liquid droplets in nanoliter scale [4]. The method goes under the name acoustic droplet ejection (ADE) and is able to transfer droplets down to 2.5 nanoliter from a source well to a destination well.

Upon dissolution the CM group stores the samples in 80 μl tubes that are compatible with the acoustic liquid handler. An order is placed through a template that specifies how the assay ready plate should be delivered when considering which compounds should be included and in what volume. The source plate is then created by picking the desired tubes from the chemical library. The liquid handler measures the fluid height in each of the source tubes by utilizing the different echoes from an audit sound signal. It is then possible to determine, by knowing the approximate viscosity of the solvent, what intensity (dB) that has to be applied for transferring the desired solution one droplet at a time [4].

The innovative ADE technique for liquid handling has proven successful globally in the AstraZeneca laboratories. Low volumes of liquid samples are transferred to assay ready plates in completely automated processes, increasing the throughput for biology screening. However, new techniques rarely come without complications. Since implementation, there has been a significant build-up of samples that are incompatible with acoustic dispensing. These samples are manually removed from the chemical library and thus they become unavailable for further screening, slowing down the process of drug discovery and development. By visual inspection the samples seem to have a common factor. Their tendency to be insoluble in DMSO seems to correlate the samples to each other and hinders them from proceeding in drug discovery and development.

This project aims to correlate the sample composition of 50 compounds in DMSO to the failure in acoustic dispensing. The compounds will be characterized by the shape and size of the precipitate particles, as well as any correlations amongst their chemical structure will be noted if such similarities exist. Further on, the aim of the project is to determine if the precipitate truly is the original compound or if the samples are contaminated by external means or by any chemical reaction. The aim extends to modelling the acquired samples with polymer microspheres in aquesous suspension, in order to reach a general conclusion regarding the possibility to dispense a sample that contains a solid content. With the knowledge gained from this project, the aim on a larger scope is to conclude whether the existing workflow should and can be modified for samples that precipitate in DMSO.

2

Theory

2.1 Dissolving compounds

2.1.1 Breaking down the dissolution process

Many biochemical assays are compatible and optimized for sample solutions, but dissolving a compound might not always be an easy task. An easy way to explain the dissolution process is to consider mixing sugar, i.e. glucose ($C_6H_{12}O_6$), with water [6]. One single sugar crystal in a glass of water will find itself exposed and surrounded to many water molecules. The moleules on the crystal surface will start to interact with the surrounding water molecules by intermolecular forces, in this specific case the interactions occur mainly by hydrogen bonding. At the same time the surface glucose molecules are held back by their bonding interactions with the bulk glucose molecules. If the interactions between the water molecules and the sugar surface molecules are comparably strong to the ones between the surface- and the bulk sugar molecules, the surface molecules can drift into solution and get completely surrounded by water. The glucose crystal will then loose its old surface molecules but new sugar molecules from the bulk become exposed to the water instead. When all sugar molecules are separated from each other by interactions with water molecules the sugar is considered to be completely dissolved. Adding more sugar and keeping the amount of water constant will eventually have all the water molecules consumed by interacting with sugar molecules, and when exceeding a certain threshold of sugar molecules the water is unable to separate more sugar molecules from each other. The solution has become saturated, and the solvent is unable to dissolve more of the solute under the specific physical conditions [6].

When referring to a solute as soluble, the qualitative measurement implies that the solute is fully miscible in the solvent of choice [7]. However, it is also possible to refer to compounds as poorly soluble or even insoluble. Qualitatively these two cases imply that the solvent must be present in great excess to dissolve the solid or the solid is realistically not possible to dissolve with the chosen solvent. In quantitative descriptions, the solubility is expressed as a concentration by either mass, molarity, molality etc. A common encounter is the unit molar (M) which describes the number of moles of solute that is dissolved per unit volume (dm^3) of solvent.

2.1.2 Chemical nature of the solvent

The solute-solute interactions are best replaced by solute-solvent interactions if the solvent is able to mimic the previous intermolecular interactions [6]. As for example, to dissolve a solute where the solute molecules are held together by hydrogen bonding, the solvent of choice should also form hydrogen bonds. On the other hand, if the solute molecules are held together by dispersion forces, the solvent molecules should also be held together by dispersion forces. This comes down to one of the most common principles of chemistry, the like-dissolves-like principle, which states that in order to mimic the solute-solute interactions, and thus dissolve the substance, the solvent must be of similar chemical nature as the solute. Hence polar solutes are best dissolved by polar solvents and vice versa. This is commonly illustrated by mixing water and oil without any agitation. Water is polar and oil is non-polar and thus insoluble in water. Hence the mixture phase separates in two layers due to the difference in density between oil and water.

2.1.3 Thermodynamics and kinetics of dissolution

Dissolution is a dynamic process, where the solute is kept at an equilibrium between a dissolved state and a phase joined state, by e.g. solid precipitation [6]. The equilibrium is affected by numerous external parameters, some of which are e.g. chemical properties of the solvent, temperature, pressure and pH. Stirring and shaking the solution does not increase solubility. However, the increased turnover of solvent molecules at the surface of the substance increases the dissolution rate which can be expressed by the Noyes-Whitney equation

$$r_d = -\frac{dm}{Vdt} = k_d S(C_s - C_b) \tag{2.1}$$

where k_d is the diffusion constant, S is the surface area of undissolved crystals per unit volume of the solution, C_s is the concentration of the solute at the interface of the crystal and C_b is the concentration of the bulk solution [8].

To determine if a solid spontaneously dissolves in a solvent the change in Gibb's free energy must be considered

$$\Delta G = \Delta H - T\Delta S \tag{2.2}$$

Dissolution is a process of two steps, the first step requires the solute molecules to be separated from each others interactions and the second step is to interact with surrounding solvent molecules. Each step is accompanied by an enthalpy change. The so-called lattice enthalpy (ΔH_l) is related to breaking solute-solute interactions which always require some energy, making the first step endothermic. Hence the lattice enthalpy is positive. The so-called enthalpy of hydration (ΔH_{hyd}) is related to forming the solute-solvent interactions. Forming the new interactions between the solvent and the solute can be either an endothermic process or an exothermic

process. Hence the overall enthalpy related to dissolution can be both positive or negative, which is why some solutions give away heat whilst others appear as cold when dissolving a substance. For a solid to dissolve spontaneously the Gibb's free energy must be negative. The entropy change is in most cases positive when dissolving a solid, as the disorder of the system increases. Hence the entropic contribution to the Gibb's free energy ($-T\Delta S$) is negative. If the enthalpic contribution is negative the dissolution process will most likely be spontaneous, as both the enthalpic and entropic contributions are negative and thus the Gibb's free energy becomes negative. If however, the enthalpic contribution is positive, the entropic contribution must be negative enough to overcome the enthalpic contribution, so that the Gibb's free energy becomes negative. In some special cases the entropy of the system may decrease when dissolving a solid, which is due to the solvent molecules forming cage-like structures around the solute molecules. As such, these special situation result in a positive $-T\Delta S$ which requires a negative enough enthalpic contribution to achieve spontaneous dissolution.

Considering the entropic contribution it is clear that the temperature can be altered to make the dissolution spontaneous. A solid that does not dissolve spontaneously at, e.g. room temperature, may dissolve spontaneously at a higher temperature as $-T\Delta S$ becomes more negative.

2.2 Moving liquids with sound

2.2.1 Acoustic waves

Acoustic waves are mechanical oscillations of pressure, travelling through a medium by periodically transferring energy from one point to another [9]. They can be illustrated as sinusoidal waves, as depicted in Figure 2.1, that oscillate between a maximum pressure, also called crest, and a minimum pressure that is referred to as through. The distance between two crests, or equivalently from through to through, is known as the wavelength (λ) and the time it takes for a wave to oscillate once is known as the period (T). Waves are commonly known to oscillate with a certain frequency (f), defined as the inverse of the period.

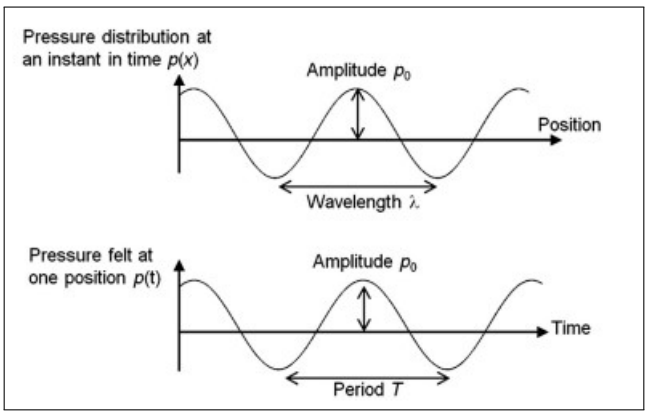

Figure 2.1: Description of an acoustic wave. Used with permission [10].

Acoustic waves require a medium for propagation, such as a solid or a fluid (both liquids and gases) and are unable to propagate through vacuum. This is because the propagation of the wave is dependent on molecular movements in the medium. An acoustic wave propagates by densifying and rarefying the medium molecules with its periodical pressure oscillation, as illustrated in Figure 2.2 below. When the pressure increases, the molecules of the propagation medium are packed more dense, reaching a maximum density at each crest. When the pressure decreases, the distance between the molecules increases and reaches a maximum distance at each through of an oscillating wave. As the molecules are compressed and rarefied the wave propagates through the medium over so-called compression and rarefaction zones. These types of waves are referred to as longitudinal waves, and are also commonly known as compression waves.

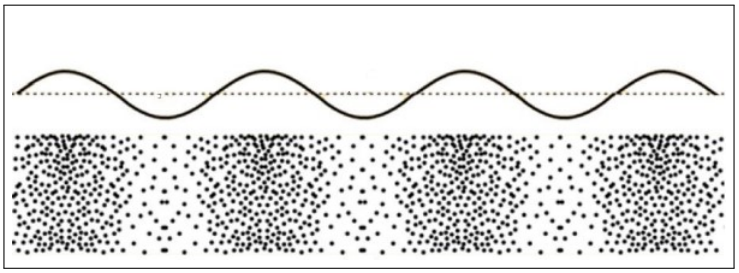

Figure 2.2: Propagation of a longitudinal wave through a propagation medium. Used with permission [11].

The velocity with which the acoustic wave propagates is dependent on the propagation medium [10]. The inertia and the intermolecular strength is affecting how well and how rapidly the wave can propagate [9]. As for example, the heavier the medium molecule, the more inertia will it have and thus can the wave propagate faster. Similarly, the stronger the intermolecular interactions, the faster can the vibrations be passed on between the molecules and the wave can propagate faster. The sound velocity, v (m/s), of a given propagation medium can be determined as follows

$$v = \frac{1}{\sqrt{\kappa\rho}} \tag{2.3}$$

where κ is the adiabatic compressibility (m^2/N) and ρ is the density of the propagation medium (kg/m^3) [10]. The surrounding physical conditions are also of importance. Consider a temperature increase as an example, the molecules will have a greater energy and are therefore able to transmit the movement of the wave faster. Hence the sound velocity in a given medium increases with increasing temperature.

Acoustic waves keep propagating until they encounter an interface between two propagation medium [10]. This could be, e.g. a liquid-solid interface, a liquid-liquid interface or a liquid-gas interface. Consider the interface in Figure 2.3 between medium 1 and medium 2, where the propagation medium have distinctly different densities and sound velocities (v_1, ρ_1, v_2 and ρ_2). The propagating wave travels from medium 1 with an amplitude A_i at normal incidence to the interface.

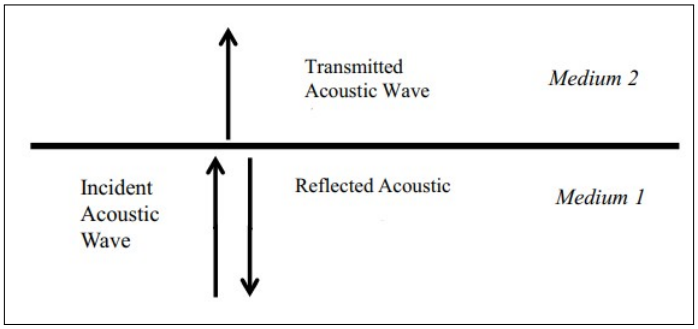

Figure 2.3: Interface between two different propagation medium for acoustic waves. Used with permission. [12].

This type of interface is characterized by the so-called acoustic impedance (Z) of the two propagation medium [10]. The acoustic impedance is a measure of how much movement an acoustic wave can generate in a medium, and is defined as follows

$$Z = \rho v \tag{2.4}$$

The acoustic impedance can be used to determine the reflection coefficient (R), which is the fraction of the incident wave amplitude that is reflected back to medium 1 at an interface, such as the interface described in Figure 2.3. The reflection coefficient is defined as follows

$$R = \frac{Z_2 - Z_1}{Z_2 + Z_1} \tag{2.5}$$

and the amplitude of the reflected wave is determined by

$$A_r = A_i \times R = A_i \times \frac{Z_2 - Z_1}{Z_2 + Z_1} \tag{2.6}$$

where A_i and A_r are the amplitudes of the incident wave and the reflected wave, respectively. Equations 2.5 and 2.6 show that the larger the difference in acoustic impedance between the two medium, the larger is the reflection of the acoustic wave [10]. However, it is important to consider the incident angle which in this case is normal to the interface. The reflection properties can drastically change as the incident angle is changed, due to e.g. critical angles that cause complete internal reflection or generation of surface waves.

The interaction of an acoustic wave with an interface is dominated by reflection in the situation where the length scale of the boundary or bounded object is much greater than the wavelength of the acoustic wave ($l >> \lambda$) [10]. If the length scale of the boundary or bounded object is in a similar length scale ($l \simeq \lambda$) or smaller than the wavelength ($l < \lambda$), the interaction becomes dominated by scattering of the acoustic wave at the interface. The scattering is dependent on both the size and shape of the scattering object. A factor ka is defined for determining whether the interaction between an acoustic wave and a spherical object is dominated by reflection or scattering.

$$ka = \frac{2\pi r}{\lambda} \tag{2.7}$$

where r is the radius of the sphere (m). If $ka >> 1$ the interaction is dominated by reflection, as depicted to the left in Figure 2.4, and if $ka << 1$ the interaction is dominated by scattering which is depicted to the right in Figure 2.4.

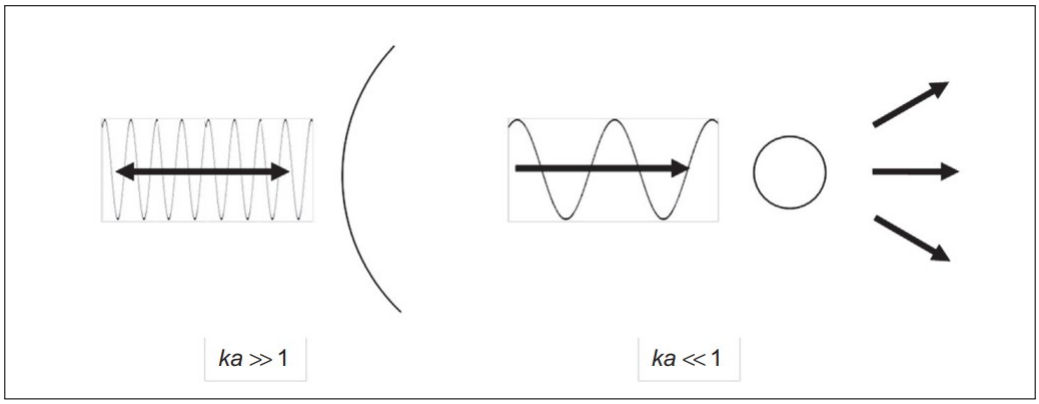

Figure 2.4: The interaction between an acoustic wave and an interface of a spherical scattering object, when reflection dominates (left) and when scattering dominates (right). Used with permission [10].

2.2.2 Creating sound

An electro acoustic transdudcer (EAT) can transform electric voltage to acoustic signals in different propagation medium [13]. The transformation normally occurs in two steps, as depicted in Figure 2.5. The first conversion is from an electric signal to fluctuations of a mechanical system, commonly referred to as an electromechanical transformation. In the second step the mechanical fluctuations cause the movement of the propagation medium to create a sound field. Commonly the transducers contain a piezoelectric constituent. Piezoelectric materials have an electric polarization related to the mechanical pressure meaning that applying a voltage will cause the material to deform and the other way around, deforming the material will generate a voltage. It is thus possible to construct reversible transducers that create an acoustic signal by applying a voltage, and detect any returning reflections by deforming the piezoelectric material and causing an electric response.

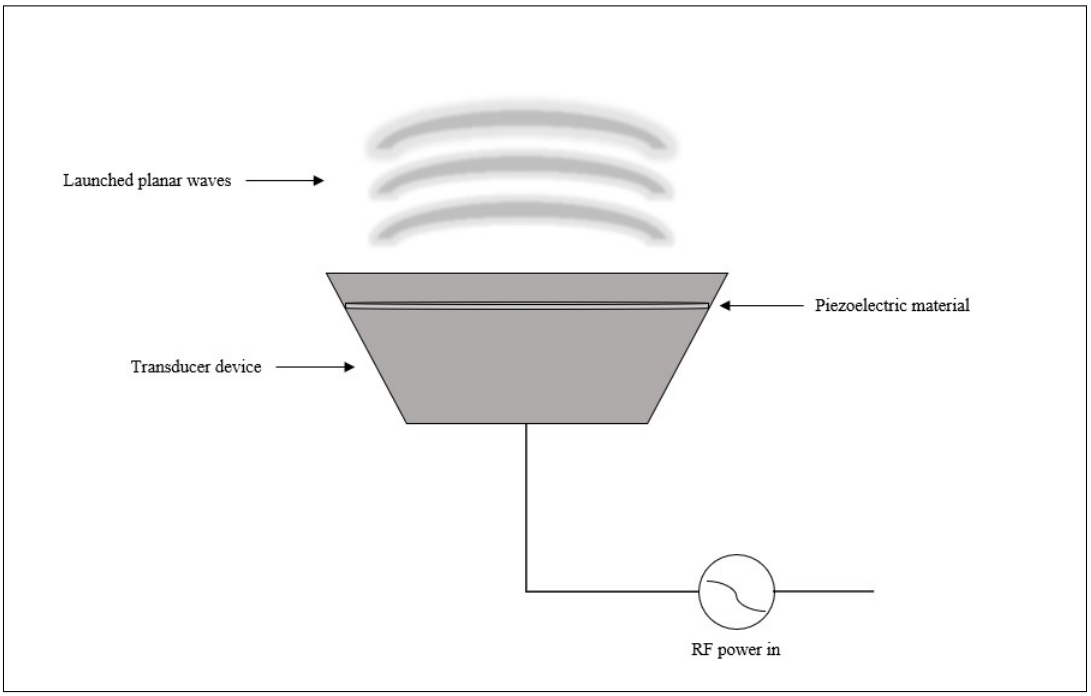

Figure 2.5: Acoustic transducer. A voltage is applied to the transducer device, causing a piezoelectric material to deform in fluctuations which generates acoustic waves that can propagate through a suitable medium. Own work, inspired by [13].

2.2.3 Principles of acoustic droplet ejection

Acoustic droplet ejection emerged as a liquid transfer method in life science during the 21st century [12]. By overcoming the restraining force of the liquid surface tension, ADE uses sound waves to accurately transfer precise volumes of liquids to assay ready destination plates. The basic configuration of ADE is illustrated in Figure 2.6. An electric radio frequency (RF) signal is applied to a transducer which converts it into ultrasonic waves, typically within a frequency range of 1 - 200 MHz. The transducer is immersed in a so-called coupling fluid (typically water) which acts as a propagation medium for the acoustic waves between the transducer and the source of the fluid that is to be transferred. A lens of specific focal length (F) and aperture diameter (D) is used to focus the acoustic field on the liquid surface. The ratio (F/D), commonly known as the F-number ($F\#$), is a measure of how sharply the acoustic signal is focused. Typically the F-number is kept close to 1 which results in a diameter of the ejected droplet (d) close to the diameter of the ultrasonic beam at the liquid surface, also referred to as the focal spot size (d_a).

If the signal is of sufficiently high intensity to overcome the surface tension of the liquid a mound is formed on the liquid surface and when the intensity exceeds a critical threshold energy a droplet is ejected.

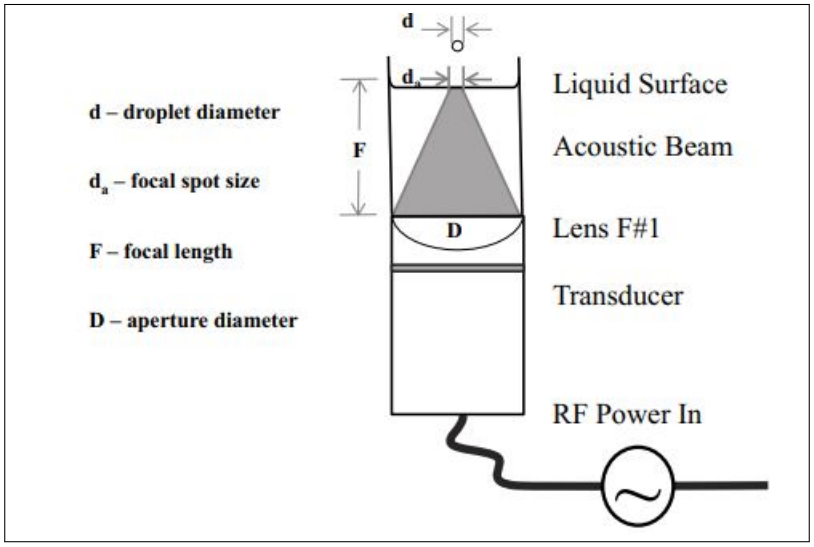

Figure 2.6: Basic ADE configuration. Used with permission [12].

2.2.4 Auditing

To determine the required intensity that is necessary for ejecting a droplet the fluid height in each source well must be determined in an auditing step [12]. It is of great importance that the audit is rapid to achieve a high throughput in liquid transfer from multiple wells. During the audit the transducer focuses one acoustic pulse, a so-called ping, from below each well of the plate. The ping propagates through the coupling fluid and causes three reflections per well, as depicted in Figure 2.7. The reflections occur at the interfaces between the coupling fluid and the well bottom (BB), the well bottom and the well fluid (TB) and between the well fluid and the free surface of the well (SR).

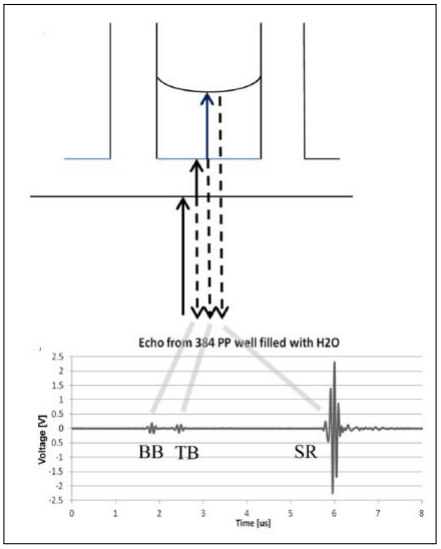

Figure 2.7: Typical audit cycle. Used with permission [12].

At each interface a fraction of the acoustic signal is reflected and recorded by the transducer. The time difference between the TB and the SR reflections is representative for the time the acoustic signal resides in the well fluid, i.e. the time it takes for it to travel to the top of the well fluid and back to the transducer. If the sound velocity in the well fluid is known, normally assumed to be the sound velocity in the solvent, it is possible to determine the height of the fluid in each well.

2.2.5 Droplet ejection

When using acoustics, there is a power threshold for drop ejection. No droplets are ejected if the RF power input is lower than a critical value. Increasing the RF power above the threshold results in droplet ejection. Each ejected drop must travel 25 mm between the source plate to the destination plate, in order to avoid failed transfer due to viscous drag and gravitational forces. A drop velocity of 1 m/s has proven to be a good target velocity, any further power increase results in secondary drops that tend to disturb the ADE precision and poses a contamination risk [12]. Hence it is of importance to apply an acoustic power, such that the received power at the focal spot of a well is sufficient for upwards droplet ejection and lower than the intensity for generating secondary droplets.

2.2.6 Dynamic fluid analysis

Dynamic fluid analysis (DFA) is a method that enables precise determination of the required acoustic energy for droplet ejection [12]. It is used to obtain an external calibration for a solvent of choice, i.e. it is not neccessary to perform a DFA before each ADE transfer.

The DFA measurement starts with a fluid height measurement as described previously. Once the fluid height is known a so-called subejection toneburst signal is ejected to the fluid, which is a ping with 2 - 3 dB lower intensity than the threshold for droplet ejection. The subejection signal perturbs the well surface and creates a mound, as depicted to the left in Figure 2.8. As the signal is below the ejection threshold the mound will rise and fall without ejecting any droplets. At a fixed time shortly after the formation of the mound another ping is ejected. This secondary signal will interact with the mound during a microsecond long period, during which the mound can be considered as static. If the mound size is large enough it splits the SR reflection to three distinctly different components, as seen to the bottom right in Figure 2.8.

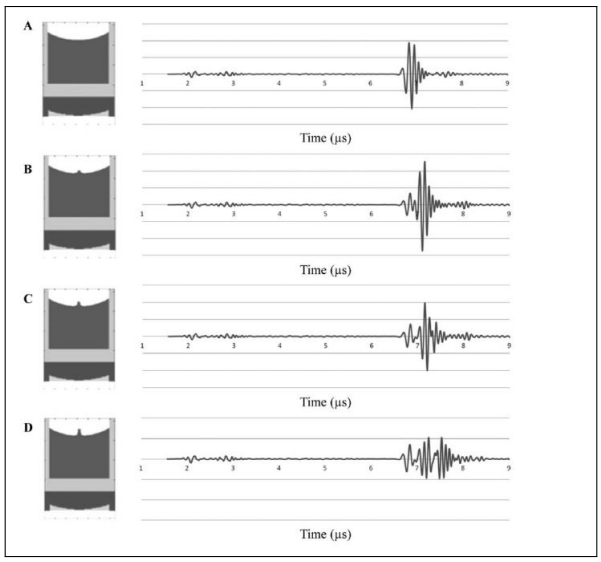

Figure 2.8: Cross sections of four fluid containing wells (A - D) for a 3D acoustic propagation simulation (left) and their respective waveform (right). The mound height progressively increases in the cross sections from A - D, showing that the mound eventually splits the SR reflecting signal into three distinct components. Used with permission [12].

The first component of the SR split signal is associated with the fluid surface completely unperturbed, hence it is often neglected in the further steps of DFA. The third and second components on the other hand, are related to the actual size of the mound. Thus they can be helpful, together with the known RF signal input, in determining the right amount of energy that is required for droplet ejection. It is convenient to use a fast Fourier transform (FFT) to convert the SR split signal to the frequency-space, as illustrated in Figure 2.9.

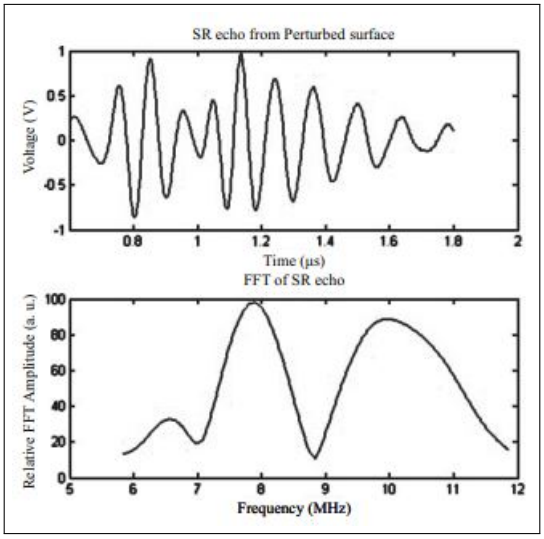

Figure 2.9: FFT of split SR reflected signal from time to frequency space. Used with permission [12].

Figure 2.9 shows a split SR reflection together with its FFT to the frequency space, which clearly shows two minima at 7.0 and 8.9 MHz. The time separation between the minima corresponds to the size of the mound. By measuring the mound size at different toneburst energies, i.e. intensities, it is possible to obtain a calibration curve similar to the one illustrated in Figure 2.10, where the logarithm of the minima spacing is related to the toneburst energy. A linear relationship can be observed, making it possible to use a series of measurements to determine the energy required for droplet ejection.

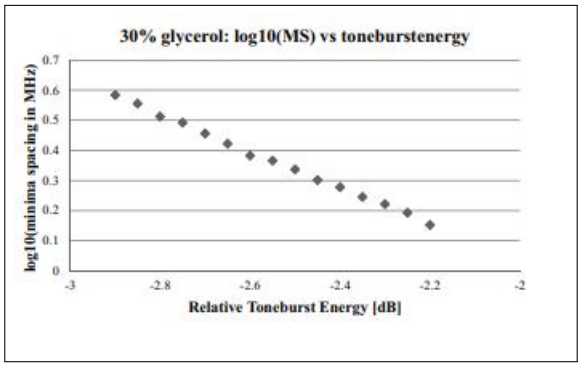

Figure 2.10: Linear relationship between minima spacing in a split SR reflected signal as a function of increasing toneburst energy. Used with permission [12].

The minima spacing that correlates to the ejection of a droplet can be determined by the following equation [12]

$$10 \times log_{10}(E_{DFA}/E_{threshold}) = A \times log_{10}(M_S) + B \tag{2.8}$$

where M_S is the minima spacing in MHz, E_{DFA} is the toneburst energy from any DFA measurement in dB, and $E_{threshold}$ is the threshold toneburst energy in dB. The constants A and B are characteristic for a fluid, and once determined they can be used in any determination of the accurate energy required for droplet ejecton. The combination of auditing and DFA has proven to be an excellent, and time efficient method for accurate determination of the supply of acoustic energy for droplet ejection in a variety of fluids.

2.3 Liquid chromatography

Liquid chromatography (LC) is a separation method that utilizes a liquid mobile phase together with a solid stationary phase, which is most commonly packed in a column [14]. An LC setup requires a pump to move the mobile phase through the system. The mobile phase itself is commonly a mix of two solvents, A and B, with one solvent being more polar than the other. By mixing the solvents in different compositions the characteristics of the mobile phase can be altered. An autosampler injects the sample to the mobile phase, and normally consists of a syringe that draws the sample and injects it into a loop. The loop itself can be filled completely, but also partially before switching the valve to let the mobile phase flow through and collect the sample. The mobile phase carries the sample through the column, in which the separation occurs. The separation itself is based on partitioning of the analytes between the two phases [15] [16]. The analyte establishes a dynamic equilibrium between the mobile and stationary phases over the length of the column, and it partitions between the phases depending on how well it prefers to stay in the respective phase. A polar analyte will rather reside in a polar phase so it partitions more into the more polar of phases, and vice versa. After eluting, a suitable detector is selected to detect the analytes and the data can then be processed in a software.

There are two main modes for running an LC, the reverse phase (RP) and the normal phase (NP) [14]. The most common is RP in which the stationary phase is less polar, and the mobile phase is the more polar of the two phases. Hence the less polar the analyte is, the more will it partition into the stationary phase and the longer time will it take to elute. Therefore, RP LC results in that the most polar analytes elute first, followed by analytes with reduced polarity. The opposite applies for NP LC

To achieve a more rapid elution for late eluting analytes it is common to apply so-called gradient elution, in which the composition of the mobile phase changes throughout the run by applying different mixtures of the solvents A and B [14]. In RP LC this implies that the composition of the mobile phase gradually changes so that the mobile phase becomes less polar, facilitating elution of the less polar analytes that are otherwise comfortable in the stationary phase. Gradient elution also allows for better resolution and sharper peaks.

Spectrophotometric detectors are common to use together with an LC setup as most solutes absorb light within the ultraviolet and visible (UV-Vis) region of the spectrum [14]. The absorption measurement requires a light source, a wavelength selector, a position for the sample to flow through and a detector. When the analyte elutes from the column it is passed through the detector. The light source emits white light and the wavelength selector can select which wavelength that is measured. The light intensity before passing the sample is known, and by measuring the light intensity after passing through the sample the absorption can be determined according to the following relationship

$$A = log\left(\frac{I_0}{I}\right) \tag{2.9}$$

where I_0 is the emitted light intensity and I is the light intensity after passing through the sample. The absorbance (A) is directly proportional to the sample concentration, as defined by Lambert-Beer's law

$$A = \epsilon bc \tag{2.10}$$

where ϵ is the compound specific molar absorptivity ($M^{-1}cm^{-1}$), b is the length of the light path through the sample (cm) and c is the concentration (M).

2.4 Mass spectrometry

Mass spectrometry (MS) can be used for measuring the the mass to charge ratio (m/z) of molecular ions, and is suitable for small molecules [14]. A MS instrumentation includes three main components, the ionization source, the mass analyzer and the detector [15]. The ionization source is responsible for producing the molecular ions and generally the ionization sources are divided into soft and hard sources. Soft ionization sources generate molecular ions without significant fragmentation, whilst the hard ionization sources cause significant fragmentation. Electrospray ionization (ESI) is a common ionization source in coupled LC-MS systems. It is a soft source where the eluting analyte passes through a needle that is kept at a few kV voltage. The electric field, caused by the voltage, at the needle tip disperses the liquid to a spray of charged droplets. The solvent is evaporated by adding a dryer gas, typically nitrogen, and in a series of evaporation steps the analyte itself will eventually obtain the surface charge. The charged analyte is then accelerated and guided by a magnetic field towards the detector, e.g. a time of flight (TOF) detector [15]. A TOF consists of an evacuated tube with the source on one end and the actual detector on the other end, such as a UV detector described in the previous section [14]. There is no further acceleration in the TOF tube, and all ions enter with the same kinetic energy. However the ions will travel the linear path to the detector in different velocity due to having different mass. Lighter ions will have a greater velocity and reach the detector faster than the heavier ions do. This way the MS can separate the ions from the ion source and the detector measures a signal that is proportional to the number of ions with a certain m/z ratio.

3

Methods

3.1 Method development

3.1.1 Sample characterization

A set of 50 substances was obtained in transparent 1 ml plastic vials. All substances were suspensions with a layer of solid content on the vial bottoms. The samples were inspected through a Zeiss® Stemi SV 11 optical microscope to determine shape and size of the precipitate particles. A polarizing filter was used to determine if the precipitates scatter polarized light in order to determine whether a precipitate was amorphous or crystalline. The precipitates were recorded with a Leica® M205 C digital microscope.

3.1.2 Volume check

Each sample was transferred from the 1 ml vials to separate acoustic tubes with a pipette. The pipette was immersed into the vials and by pipette mixing the suspensions were homogenized before 80 μl was transferred to the acoustic tubes. After sealing the acoustic tubes with caps they were placed on a 96-well rack and loaded to an automated liquid handler system. The rack was moved to a centrifuge that spun the rack for 20 seconds at 1234 RPM to even out the shape of the liquid surface which facilitates more precise measurements. After the centrifuge the rack was placed in an Echo® 550 acoustic liquid handler to measure the volume in each tube of the rack, according to the audit procedure described in the theory section. The centrifuge - volume measurement cycle was repeated a total of 50 times, with approximately 24 h difference between the first 25, and the last 25 measurement cycles in order to determine whether time is of importance.

3.1.3 Repeated testing

In an attempt to reproduce the previous volume measurements, 50 new acoustic tubes were acquired. The interior of the empty acoustic tubes was inspected with a Dino-Lite® premier digital microscope to assure that the inner surface of the tubes had no significant effect on the audit measurement. Shallow scratches were observed in all tubes, and is thus considered to have no severe effect on the audit. No deep scratches were observed. In contrast to the initial testing, the sample vials were

shaken at 250 Hz for 10 min with a table top shaker for mixing. Additional homogenization was performed with a pipette before transferring 30 μl of each substance to the inspected acoustic tubes. The sample volume in the repeated experiment was lower compared to the previous experiment due to low sample availability, and to assure that all acoustic tubes were filled with the same sample volume. The acoustic tubes were sealed and placed in a 96-well tube holder rack that was centrifuged for 1 min at 1000 RPM. The tubes were de-capped and the content was inspected with a Dino-lite® premier digital microscope, in order to see how the sample content distributed within the tubes. The tubes where then sealed with the same caps again, and loaded into the automated system where they were subjected to one volume measurement cycle as described earlier.

3.1.4 LC-MS method development

A new compound was acquired (AZ12175302) for the LC-MS method development due to its significantly higher sample availability and due to its solubility in DMSO. A 10 mM stock solution was prepared by dissolving 1.12 mg of AZ12175302 in DMSO to a final volume of 331.25 μl. The weighing was performed by hand, and the dissolution with the help of a Tecan® freedom EVO automated liquid handler.

From the stock solution 200 μl was transferred to a 1 ml transparent plastic vial with a 20 - 200 μl Eppendorf pipette, serving as the stock for a dilution series. A total of four solutions were created by repeatedly diluting the previous solution in 1:2 ratio with DMSO, all with the same 10 - 100 μl pipette. That is, 100 μl of the 10 mM solution was transferred from the vial containing 200 μl to a new vial, to be diluted with 100 μl DMSO to a final concentration of 5 mM. The same procedure was performed on the new 5 mM solution to obtain a 2.5 mM solution, and finally the procedure was repeated to obtain a 1.25 mM solution. The dilution procedure was performed this way in order to avoid changes in pipette equipment so that the settings remain constant.

Four wells in a 96-well polypropylene plate were filled with 50 μl of 10 mM, 5 mM, 2.5 mM and 1.25 mM solutions of AZ1217530, respectively. The plate was sealed with an automatic sealer and placed in a Waters® ACQUITY Arc UPLC system. The sample was kept at 20 °C in the system sample manager until analysis and between each injection. Seven injections were performed for each solution with partial loop filling through a 2 μl loop, starting with an injection volume of 0.4 μl and increasing the volume with 0.1 μl per injection up to 1 μl. The injections were set according to the recommendations that the loop is to be used with between 20 - 50 % of its volume during partial loop injections.

The HPLC system was operated in an acidic reverse phase method with an ACQUITY UPLC HSS C18 chemistry column. The column temperature was set to 60 °C. Acidic mobile phases were prepared in 1000 ml glass flasks and were spiked with a pH 3 acidic stock solution. Each injection had a run time of 2 min with a constant flow rate of 1 ml/min. The mobile phase gradient was set from 90/10 (water/acetonitrile) to 1/99. Each injection was followed up by a rinse with 600 μl

of weak wash and 200 μl of strong wash, and between each injection a 1 μl DMSO blank injection was run through the column.

Mobile phase-, acidic stock-, weak wash-, and strong wash compositions can all be found in Appendix 1 in Table A.1, Table A.2, Table A.3 and Table A.4 respectively. The mobile phase gradient is displayed in Table A.5 in Appendix 1, as well as relevant temperatures and autosampler settings are found in Table A.6 and A.7, respectively.

The detection of the compound was performed with a spectrophotometric detector, by UV absorbance measurements. A scan was performed between the wavelengths of 200 - 1200 nm. The mass spectrometer was set to measure for the exact mass of the model compound in order to easily relate the absorbance peak to the compound itself. The peak area was integrated in MassLynx V4.2 SCN993 and any linear relationship between the peak area and increasing injection volume was investigated, as well as any linear relationship between the peak area and increasing concentration. The lowest suitable injection volume that worked for both 10 mM and 1.25 mM solutions was chosen for the method.

3.2 Method

3.2.1 Insolubility confirmation

The LC-MS method was applied to the 50 compounds, in order to determine whether they are insoluble in DMSO or if the precipitate is something yet unidentified. The supernatant of each compound was transferred in a volume of 30 μl to individual wells in a 96-well polypropylene plate by pipetting. The plate was sealed and placed in the LC system. One injection per sample was performed with an injection volume of 0.5 μl. Each compound was identified in the mass spectrum and the peak area was noted.

A diluted set of all 50 compounds was created by the following procedure. Each compound was homogenized by pipette mixing and 10 μl of each compound, including precipitate this time, was transferred to a new set of separate vials. The samples were then diluted with 90 μl of DMSO and shaken by a table top shaker for 10 min at 250 Hz. Most of the samples turned visually dissolved. A 96-well plate was filled with 50 μl of each compound solution. The plate was sealed and placed in the LC-MS system, where it was subjected to the same method as the non-diluted samples mentioned above. Each substance was identified in its respective mass spectrum and the peak area was noted.

The ratio between the peak area of the diluted samples and the peak area of the non-diluted samples was determined, in order to confirm if the precipitate consists of the original substance.

3.2.2 Grid survey

To determine the effect of a physical hindrance, such as a precipitate, on the propagation of the acoustic wave, polymer microparticles were used to model a precipitate. Five different sizes of poly(methyl metacrylate) (PMMA) microspheres as 10 -wt% aqueous suspensions were acquired from Micro particles GmbH®. The PMMA microsphere sizes were determined to 29.98, 60.1, 101, 127 and 148 μm, in order to cover a broad range of radii and according to the retailer availability. It was desirable to cover a broad range of sphere radii in order to reason if scattering of the sound wave or reflection was the predominate effect in signal loss. Hence to determine the effect of scattering, the wavelength of the propagating wave was determined by the following relationship

$$\lambda = \frac{v}{f} \tag{3.1}$$

where λ is the wavelength of the acoustic wave, v is the speed of sound in the propagation medium and f is the frequency (11.5 MHz in this study).

A dilution series was created from the microsphere stock suspensions by primarily transferring 200 μl of each stock suspension to a transparent 1 ml plastic vial. Then 100 μl was transferred to a new vial and diluted with 100 μl MQ water. The same procedure was performed on the new diluted suspension etc., until each stock suspension was diluted to a total of 8 aliquots, each considered to contain 50 % less spheres than the previous aliquot. Each aliquot was then transferred in a volume of 50 μl to acoustic tubes that were placed in a 96-well rack. The rack was centrifuged at 1000 RPM for 5 min to force sedimentation of the PMMA spheres in the acoustic tubes, and directly after it was placed in the automated system it was subjected to 5 consecutive volume measurements.

The acoustic liquid handler was set on standalone mode, meaning it was disconnected from the automated system, and the rack was loaded on the rack holder manually. A manual, more detailed, volume measurement was performed. The acoustic tube bottom was divided into a 41x41 grid. One acoustic ping was sent to each grid point and the echoing signal was recorded to determine the fluid height at each grid point. For each tube, the recorded signals were used to create one 2D and one 3D topography map in order to determine how the interference over acoustic tube bottom is related to the possibility of measuring the volume. The number of grid points that provided a 0-height measurement was divided by the total number of grid points to obtain a fraction of the total number of expected echoing signals, that were immeasurable.

4

Results

4.1 Precipitation characterization

By visual inspection with the naked eye, precipitation was observed in all acquired samples. Figure 4.1 displays magnified 1 μl droplets of four different suspensions, showing the presence of precipitate. The size and shape of the precipitates varies amongst the compounds. Figure 4.1b and 4.1c represent crystalline precipitates that scatter polarized light, whilst the precipitates in Figure 4.1a and 4.1d are amorphous.

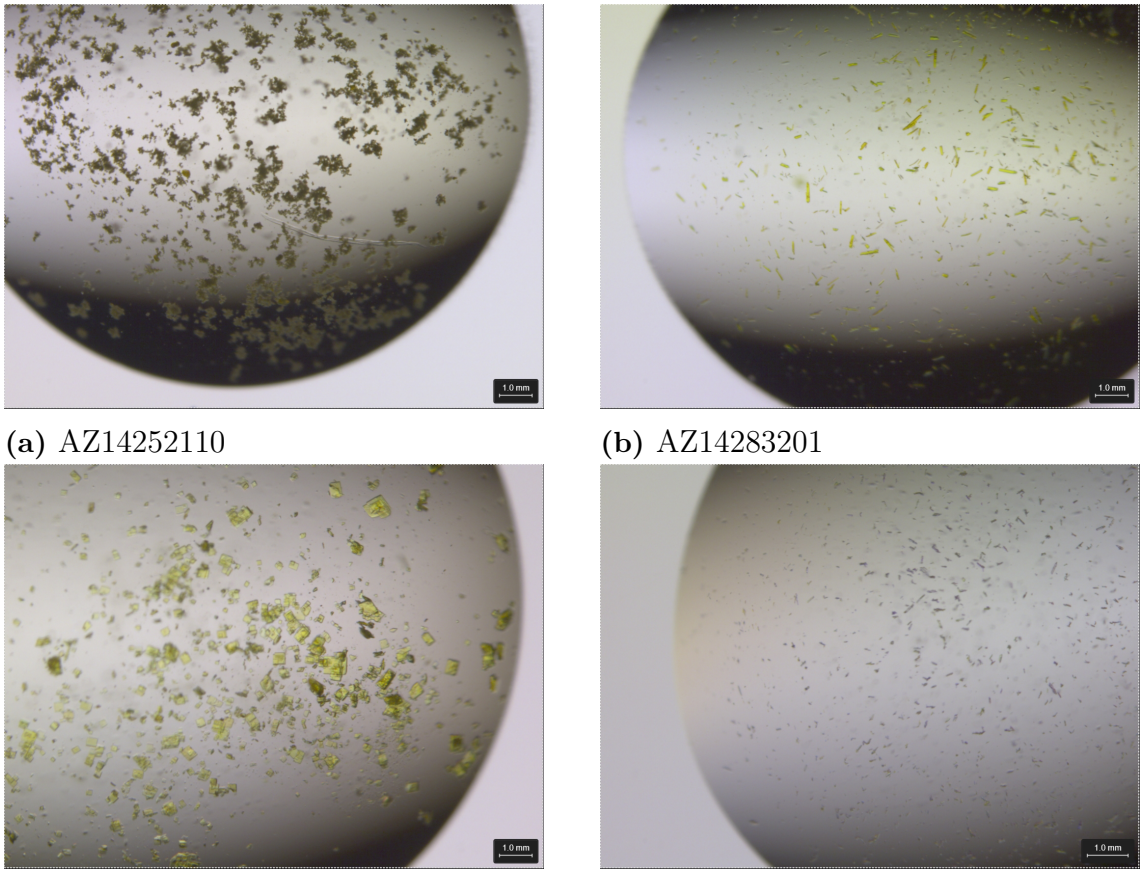

(a) AZ14252110 **(b)** AZ14283201

(c) AZ14192861 **(d)** AZ14252290

Figure 4.1: Magnification of four 1 μl droplets of different suspensions captured with digital optical microscope.

4.2 Volume measurements

During the initial 50 volume measurements it was possible to determine the volume of 43 suspensions, whilst the measurement failed for 7 of the suspensions. When the experiment was repeated with only one volume measurement, 9 suspensions that were previously measured became immeasurable. Simultaneously, 6 suspensions that failed the first measurements were measurable. Table 4.1 displays the number of successful volume measurements for 10 different compounds. The compounds left unmarked were consistent and measurable in both the first and the repeated measurement. The compounds highlighted in red showed inconsistency between the measurements. The result from the volume measurement for all 50 compounds can be found in Table B.1 in Appendix 2.

Table 4.1: List of 10 compounds with their respective number of successful volume measurements in both initial and repeated testing. The compounds highlighted in red were inconsistent between the two experiments.

Compound ID	Successful volume measurements (out of 50)	Successful volume measurement in repeated experiment (out of 1)
AZ14243461	50	1
AZ14250073	50	1
AZ14252290	50	1
AZ14260181	50	1
AZ14274477	50	1
AZ14253109	0	1
AZ14267257	0	1
AZ14340540	0	1
AZ14256291	50	0
AZ14268657	50	0

4.3 LC-MS method development

At a flow rate of 1 ml/min, a column temperature of 60 °C and a mobile phase gradient from 90/10 (water/acetonitrile) to 1/99, the model substance AZ1217530 eluted in less than 2 min. Figure 4.2 displays the relationship between the integrated peak area and increasing injection volume for 10 mM and 1.25 mM DMSO solutions of AZ1217530.

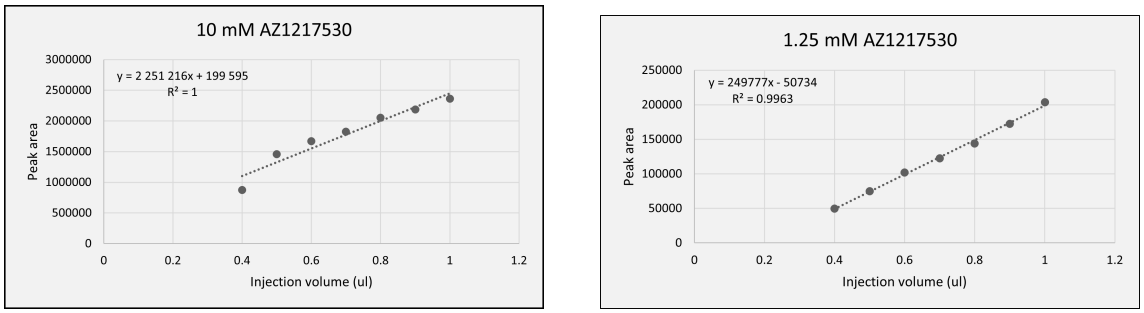

(a) **(b)**

Figure 4.2: Relationship between the integrated peak area for compound AZ1217539 in a 10 mM (a) and a 1.25 mM (b) DMSO solution and increasing injection volumes between 0.4 - 1.0 μl.

Figures 4.2a and 4.2b were used to determine that an injection volume of 0.5 μl was suitable for the method. Figure 4.3 shows that there is a linear relationship between the integrated peak area for compound AZ1217530 dissolved in DMSO and increasing concentrations between 1.25 - 10 mM for an injection volume of 0.5 μl.

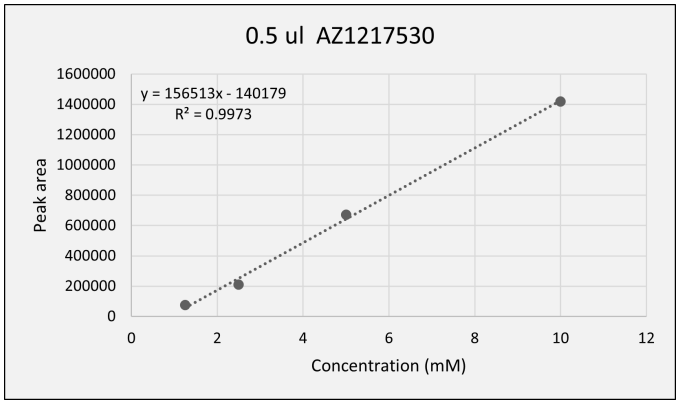

Figure 4.3: Relationship between the integrated peak area for an injection volume of 0.5 μl of compound AZ1217530 and increasing concentrations from 1.25 mM to 10 mM.

The linear relationships obtained for all concentrations and injection volumes can be found in Figure A.1 and Figure A.2 in Appendix 1.

4.4 Absorption measurements

The LC-MS method detected 49 of 50 compounds in the acquired set. The peak area ratios ranged from 0.11 (lowest) to 139 (highest). The peak area ratios for five compounds are displayed in Table 4.2 below and the peak area ratios for the complete set of compounds can be found, together with the molar mass, retention time and peak areas in Table C.1 in Appendix 3.

Table 4.2: Peak area ratio (diluted/non-diluted) for five compounds.

Compound ID	Peak area ratio
AZ10829511	0.11
AZ14177187	1.25
AZ14233546	10.33
AZ14340540	44.20
AZ14262702	139.41

4.5 Grid survey

The lowest number of 0-height measurements corresponded to 42 % of the total number of measurement points, whilst the highest number of 0-height measurements corresponded to 86 %. Both the highest and the lowest number of 0-height measurements were achieved by the spheres with 60.1 μm radius, for which the results are displayed in Table 4.3. For all sphere sizes, the number of 0-height measurements is displayed with the corresponding fraction and the possibility to measure the volume of the tube content in Appendix 4.

Table 4.3: Fraction of all measurement points that were 0-height measurements and the possibility to measure the tube content volume, for spheres with the radius 60.1 μm.

60.1		
Dilution	Fraction of interfered area	Measurable
1:1	86%	No
1:2	69%	No
1:4	71%	No
1:8	61%	Yes
1:16	47%	Yes
1:32	48%	Yes
1:64	42%	Yes
1:128	47%	Yes

For the spheres of 29.98 μm radius the volume was measurable until the 0-height measurements corresponded to 59 % of the total number of measurement points. The same number was 61 % for the spheres of 60.1 μm radius, 71 % for the spheres of 101 μm radius, 48 % for the spheres of 127 μm radius and 51 % for the spheres of 148 μm radius.

Figure 4.4 displays 2D and 3D illustrations of the grid survey measurements for the highes- and lowest achieved 0-height measurements. The blue measurement points are 0-height measurements whilst the yellow points are maximum height measurements.

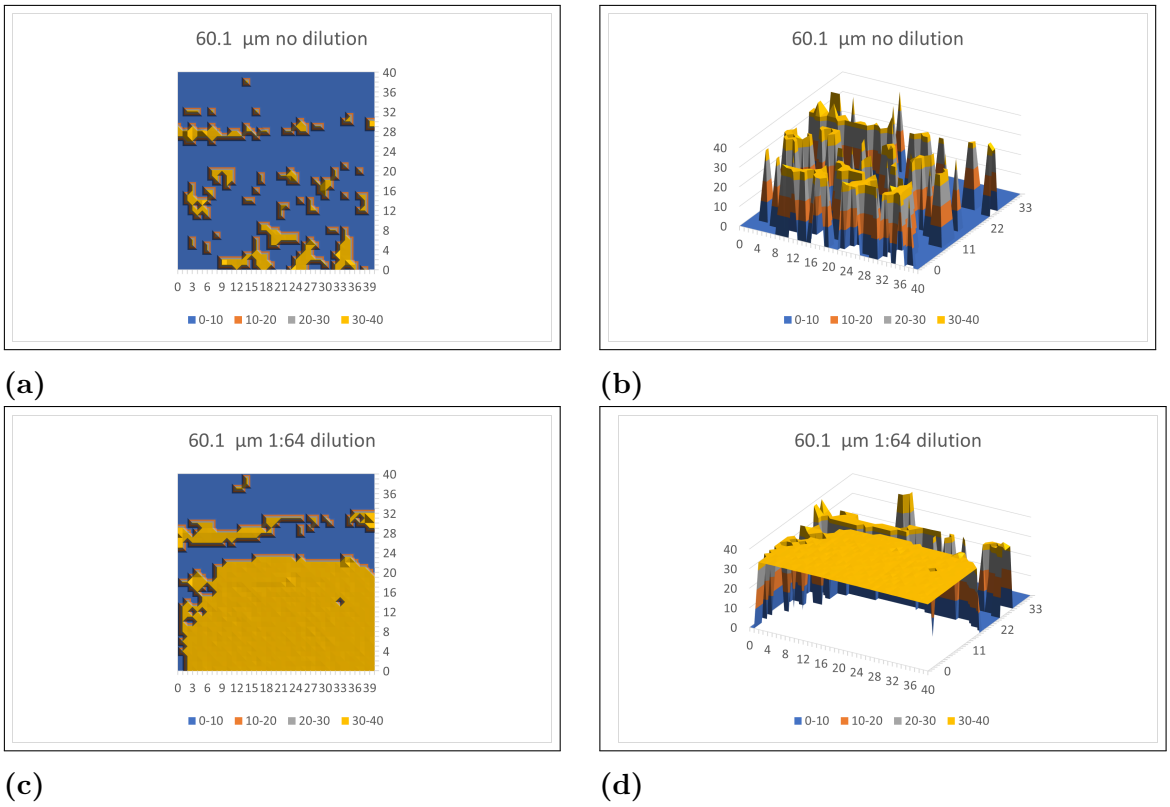

Figure 4.4: 2D and 3D illustrations of the tube content, at the highest (a and b) and the lowst (c and d) number of achieved 0-height measurements by the 60.1 μm spheres. The blue measurement points represent the height between 0-10 mm, the orange measurement points represent the height between 10-20 mm, the grey measurement points represent the height between 20-30 mm and the yellow measurement points represent the height between 30-40 mm.

A complete collection of 2D and 3D illustrations obtained from the grid survey for all sphere sizes can be found in Appendix 4.

5

Discussion

5.1 Sample characterization

As confirmed by visual inspection with both the naked eye and by magnification in a microscope, all acquired samples contained precipitation. The naked eye can be considered as an insufficient method for scientific conclusions but most often it can give useful indications that can be confirmed later on. Figure 4.1 shows four examples of precipitate, indicating that different shapes and sizes can be found in the set of compounds. Even though there are size- and shape- factors to consider in a possible interaction with an acoustic signal, the variance shown in Figure 4.1 indicates that it most probably is not the determining factor in this study. It is also notable that some of the precipitates, such as the ones in Figure 4.1b and 4.1c, scatter polarized light and can thus be considered as crystalline whilst the precipitates in Figure 4.1a and 4.1d are amorphous as they do not scatter polarized light. Hence it is also possible to assume that the problem does not arise due to if the precipitate is crystalline or not. From this reasoning, the physical characterisation of the precipitates is not expanded further, and it is believed that the bare presence of precipitates is the most affecting parameter. It is also notable that a significant variance is found amongst the chemical structures of the precipitate showing no correlation with the disturbance of the acoustic signal.

5.2 LC-MS method for compound identification

However, structure-property relationships are important as the chemical structure heavily affects the solubility in DMSO. Most probably, the largest similarity between all the compounds in this study is their poor solubility in DMSO which is related to each individual compounds chemical structure. Thus it was important to determine whether the precipitate truly is the insolubilized compound, if it is contamination or if it is a product from any chemical reaction. This is the reason for developing the LC-MS method. The initial conditions, such as sample temperature, column temperature, run time, mobile phase gradient etc. was collected from an already existing quality control routine workflow. Most important was to minimize sample use due to low sample availability, and thus to find a low injection volume compatible with both 10 mM solutions and diluted solutions. The LC-MS method was developed with a model compound, fully soluble in DMSO, to avoid any unnecessary use of

samples. As presented in the results section, 0.5 μl was chosen as the injection volume for 10 mM and 1.25 mM solutions. All the injection volumes were however consistent and showed linear relationships between the integrated peak area and the injection volumes, as displayed in Figure A.2 in Appendix 1. It is notable that 0.4 μl had a lower R^2 value (0.91) compared to the other injection volumes (0.99), but it could be an effect from the outlier from the 5 mM measurement which is clearly positioned far above the linear regression in Figure A.2a. Other than that, all other injection volumes that were tested could be used in the final method but to minimize the sample use the lowest one was chosen.

When applied to the set of compounds the LC-MS method was expected to indicate if the compounds were indeed poorly soluble in DMSO. The first measurement was performed on the supernatant only, completely neglecting the precipitate. The second measurement was performed on a homogenized diluted sample, meaning that DMSO was used to dilute a sample containing precipitate as well. This gives two possible situations, one in which the absorbance differs with a factor similar to the dilution factor and one in which the absorbance difference is higher. The samples were diluted with a factor 10, and in the case where all of the substance is initially dissolved the peak area measured for the diluted sample should be 10 times smaller than the peak area for the non-diluted sample. Any higher peak area ratio would imply that more of the substance is dissolved from the precipitate once the DMSO is added. As can be observed in Table C.1 in Appendix 3 nearly all of the 50 compounds had a peak area ratio larger than 0.10. As the peak area ratios were larger than the dilution factor and as the precipitation was dissolved upon adding DMSO it is reasonable to assume that the precipitate represents the compounds. This argument is strengthened by the fact that no other absorption peaks were observed in the mass spectra of the compounds and any contamination and chemical reactions can be neglected.

It is notable that the most peak area ratios are higher than expected. The solubility is constant if the conditions, such as pH and temperature, are unaltered. Hence it would be reasonable to expect a peak area ratio close to 1 when more of the compound is dissolved from the precipitate. The high ratios are most probably consequences from an overloaded detector. This could be due to having some precipitate left in the wells, small enough to be invisible for the naked eye, but very soluble in the mobile phase. Hence when it is carried by the mobile phase it dissolves and causes a high signal for the detector.

Three compounds, AZ14340727, AZ10829511 and AZ14335208 all had peak area ratios close to 0.10. They were measured to 0.11, 0.12 and 0.12, respectively. For the three compounds mentioned, only AZ10829511 had additional peaks in its mass spectrum other than its own peak and the DMSO peak. Thus in this individual case the precipitation could be contamination. For AZ1430727 and AZ14335208 the low ratio can be explained by non-representative sample collection. When transferring a suspension aliquot from one vial to another by pipetting there is a risk of not obtaining a sample that is representative enough. As for example, the pipette mixing can be insufficient to homogenize the sample or some precipitate might stick to the

pipette tip etc.

The vast majority of samples indicate that the suspensions are in fact saturated and without the presence of any contamination. It is therefore assumed that in the majority of cases, the synthesis is pure enough to not blame contamination for the failure in acoustic dispensing.

5.3 Volume measurement

So far the results have indicated that the chemical nature of the compounds, the size- and shape of the precipitate particles and contamination are insignificant for the failure in acoustic dispensing. As presented in the results section, and more extended in Table B.1 in Appendix 2, the volume measurements do not seem to be compound-specific as repeating a volume measurement experiment from scratch is inconsistent with the results obtained from previous experiments. It is thus reasonable to assume that the pure presence of precipitate particles is the main reason in dispensing failure, and the compound itself is of less importance.

Because of the irregularity when considering shape, size, chemical structure etc. of the compounds the experiment was continued with monodisperse PMMA microspheres in aqueous suspension. In accordance to previous observations, the presence of a solid (i.e. the PMMA spheres) managed to disturb the signal in a way that cancelled the volume measurement. It was also shown that some dilutions of the suspension were measurable which is consistent with the result from measuring the set of compounds, which confirms that the acoustic signal manages to reach the detector in some cases even though there is a precipitate present.

5.4 Grid survey

The grid survey was performed to investigate if there was any correlation between failing a measurement and the fraction of measurement points that are unable to give a signal back to the detector. It is notable that even though the sphere suspensions are diluted the maximum fraction of missing signals levels out around 45 %, indicating that a more severe interference is difficult to achieve with the available equipment.

It is important to highlight the inconsistency in succeeding with a volume measurement related to the fraction of measurement points that are immeasurable amongst the different sphere sizes. As for example, no volume measurement failed when the 0-height measurements corresponded to a lower fraction than 47 % of the total measurement points. The upper limit varies amongst the different sphere sizes. As for example, it was impossible to determine the volume for the tube containing spheres of 29.98 μm radius when the number of 0-height measurements corresponded to 58 % of the total number of measurement points but it was possible to determine the volume for the tube containing spheres of 60.1 μm with 61 % 0-height measurements. Hence the grid survey does not provide any interference threshold limits, but rather

indicates that if there is a certain amount of precipitate present and it interferes the acoustic signal enough the measurement is not possible to proceed with. It is also reasonable to believe that the position of the precipitate on the tube bottom is of importance. Locating just a small amount of the precipitate at the focus point of the volume measurement signal can be enough to make the volume immeasurable.

The attempt to model the inner tube content by a 2D topography map and a 3D grid is highlighted for the two extreme cases in the results section. The full list of 2D and 3D models can be found in Figures D.1, D.2, D.3, D.4, and D.5 in Appendix 4. The blue areas in the models represent measurement points where the signal is interrupted enough to yield a 0-height measurement. The yellow areas are instead the maximum height measurements. As can be seen in the pictures, the measurable area tends to locate itself on the bottom half of the models and the non-measurable area does the opposite. This is most likely due to the centrifuging step, which does not distribute the spheres evenly over the tube bottom. Instead, they are pressed towards one end of the tube.

In an attempt to determine whether reflection or scattering of the acoustic signal is the main reason of signal loss, eq. 2.7 should be considered. The sound velocity in water is approximately 1500 m/s [17] [18] and the frequency used is in the liquid dispenser is 11.5 MHz, which gives a wavelength of approximately 130 μm according to eq. 3.1. That would give a range of ka values between 1.44 - 7.15 for the PMMA microspheres used in this study. According to the theory section, this would imply that reflection is the main source of interference with the acoustic signal by the PMMA spheres and that it is enough to cause a 0-height measurement. The acoustic impedance for PMMA is 3.25 MRayl [19] and for polypropylene and polystyrene, two common plastic materials for manufacturing consumable laboratory ware, the impedance is 1.9 and 2.52, respectively [20]. That would give reflection coefficients of 0.26 and 0.13, respectively, when a sound wave propagates from the acoustic tubes to the PMMA spheres according to eq. 2.5. These are fairly low reflection coefficients and it is expected that the detector does not interpret the reflection from the spheres as the reflection of the fluid meniscus. Hence it is reasonable to believe that both scattering and reflection might in combination be responsible for the signal loss when a 0-measurement is obtained.

5.5 Final remarks on current workflow

Lastly, to conclude the discussion the process of forcing a substance into solution should be considered. Increasing the temperature during the dissolution of small molecules might backfire. As explained in the theory section the thermodynamics of the dissolution process are favoured by increasing the temperature, favouring the dissolution process and increasing the workflow efficiency as the process accelerates. When a small molecule seems to dissolve slowly the CM department applies sonication, increasing the agitation and heating up the mixture by sound wave radiation. This has dual effect. Firstly, the solid particles are finely distributed and have a larger contact area with the solvent and secondly the solubility increases due to the increased temperature. The particles can be too small to see with the naked eye, and can even be temporarily dissolved. During storage the temperature decreases which also reduces the solubility and the finely distributed particles have time to aggregate again. As a consequence, the solution becomes saturated and the substance precipitates. The results from the study imply that the character of the precipitate is less important than its existence, making the early stages of the dissolution workflow the largest source of error for compatibilizing the samples with acoustic dispensing. Even though the acoustic dispensing may proceed with precipitates present the concentration is not guaranteed to be 10 mM, definitely not if the compound itself is precipitating which has shown to be the majority of cases.

6

Conclusion

There are obvious reasons for concluding that the presence of solid precipitate particles or solid contamination pose major problems for acoustic dispensing, which is to be expected as the method is yet to be developed and optimized for suspensions. The size and shape of different precipitates are concluded to be of less importance to the failures in acoustic dispensing. The chemical structure of the compounds is not correlated to the actual interference with the acoustic signals but has significance in the sense that the structure-property relationships makes it insoluble in DMSO, which makes the compound incompatible with acoustic dispensing as the precipitate might cause failure in the volume measurement that precedes the sample transfer.

A LC-MS method is likely to be suitable as analysis method to identify a compound in DMSO solution, and to quantify its concentration in a relative scale. Due to the lack of existing calibration methods it is not possible to determine the concentration of the supernatant. However, the LC-MS method is enough to determine whether the original compound is represented by the precipitation or if it is contamination. As most of the peak area ratios were larger than the dilution factor, and as no other peaks were observed in the mass spectra of the compounds, it is concluded that the precipitates are the same as the original compounds.

Each dispense is preceded with a volume measurement of the tube content, which this study has shown can be assumed as randomly succeeding when the sample contains precipitate. The PMMA microsphere modelling of suspensions failed to provide any thresholds for when a volume measurement fails. The conclusion is that it is most probably enough to interfere with the acoustic signal over the exact tube bottom area where the audit ping passes through. Eliminating samples with precipitate should be of greater focus than determining the threshold for a successful liquid transfer. This is mainly as the concentration of the sample cannot be guaranteed as 10 mM when there is precipitation.

Forcing a compound into solution by increasing the temperature is with high probability the simplest and most used method for substances that are difficult to dissolve, which is why it is easy to implement in a routine workflow. However, there is a major risk with this method as the sample cools down during storage and thus the compound can precipitate. This is why altering the thermodynamics by increasing the temperature can be concluded to not be the optimal method to implement in a workflow that is related to acoustic dispensing.

A final conclusion is that the problem of precipitates might not be solved in any way with the help of the acoustic dispensing instruments. Instead the focus should be shifted on how to handle the situation when a small molecule is difficult to dissolve and when it is forced into solution. The easiest solution might be to treat compounds differently depending on if they dissolve easily or if they are forced into solution by heating. An alternative workflow might be the answer to that question, which will be discussed in the following section.

7

Alternative workflow

This section aims to discuss an alternative workflow, in which substances that are difficult to dissolve are treated separately from the ones that dissolve with ease. The aim with the alternative workflow is to construct a concept method for unraveling the potential of all substances that are synthesized, even though there is a risk of precipitation. Time is of the essence in drug discovery and to keep the workflow time efficient altering the thermodynamics to increase the solubility in a given solvent should be kept as the method of choice when a compound is difficult to dissolve. It is from beyond this part of the process that the compounds should be treated different. There is a risk of precipitation when the compounds cool down during storage, as the solubility decreases again. Hence it is important to characterize the compound when it is dissolved. Expanding from the normal 10 mM solution might be an alternative, and creating a dilution series from, e.g. 1 - 10 mM is a reasonable option. The dilution series can be subjected to an analytical method, such as the LC-MS method in this study, to create an external calibration curve. As for example, relating the peak area to the concentration of the different samples in the dilution series. A simple UV-absorbance measurement with a spectrophotometer can also be applied to avoid using a more complex instrument setup. As the absorbance is proportional to the concentration, it should also be enough to perform one measurement directly on the forced 10 mM solution.

If the sample precipitates during storage the supernatant can be extracted by, e.g. centrifuging the sample and then by vacuum filtration through a fine particulate filter. When the supernatant is separated from the precipitate it can be subjected to the same analytical method again. The detected signal, e.g. absorbance or integrated peak area can then be related to a concentration with the help of the external calibration curve. When the concentration is determined the compound can be re-implemented in the normal routine workflow as a liquid sample, as it is possible to use it in the acoustic dispenser. The only difference from now is that the sample is to be treated as having a different concentration from the otherwise normal 10 mM solutions. This might however be of less importance in the final drug formulation if the substance is considered to have high potential, and hopefully this can expand the number of substances in the screening projects and thus increase the probability of finding new medicines in the future.

From a company perspective an alternative, or additional, workflow might be difficult to implement. The workflow requires resources, both physical and economical which most probably is not worth investing for a very small fraction of all synthesized compounds. Hence it might be more reasonable to use lower concentrations as a first step towards compatibilizing ADE with compounds that are poorly soluble in DMSO.

Bibliography

[1] World Health Organization. *Noncommunicable diseases*. Available at https://www.who.int/news-room/fact-sheets/detail/noncommunicable-diseases (2022/09/16).

[2] United Nations. *The 17 goals*. Available at https://sdgs.un.org/goals (2023/03/14).

[3] AstraZeneca. *Our Company*. Available at https://www.astrazeneca.com/our-company.html (2023/03/14).

[4] Sarda S. Green C.P. Spencer P.A. "Advancing automation in Compound Management: a novel industrial process underpinning drug discovery". In: *Drug Discovery Today* 26 (1 2021), pp. 5–9. DOI: 10.1016/j.drudis.2020.09.032.

[5] McCloud T.G. Waybright T.J. Britt J.R. "Overcoming problems of compound storage in DMSO: Solvent and process alternatives". In: *Journal of Biomolecular Screening* 14 (6 2009), pp. 708–715. DOI: 10.1177/1087057109335670.

[6] Laverman L. Atkins P. Jones L. *Chemical Principles: The quest for insight*. 7th ed. Macmillan Higher Education, 2012. ISBN: 9781319154196.

[7] Savjani J.K. Savjani K.T. Gajjar A.K. "Drug Solubility: Importance and Enhancement Techniques". In: *ISRN Pharmaceutics* (2012), pp. 1–10. DOI: 10.5402/2012/195727.

[8] Gao Y. Glennon B. He Y. Donnellan P. "Dissolution Kinetics of a BCS Class II Active Pharmaceutical Ingredien". In: *ACS Omega* (2021), pp. 8056–8067. DOI: 10.1021/acsomega.0c05558.

[9] Karmakar P.K. "Acoustic Wave". In: *Acoustic Waves - From Microdevices to Helioseismology* (2011), pp. 79–122. URL: http://www.intechopen.com/books/acoustic-%20waves-from-microdevices-to-helioseismology/acoustic-wave%20InTech.

[10] Watson N.J. "Ultrasound tomography". In: *Industrial Tomography: Systems and Applications* (2015), pp. 235–261. DOI: 10.1016/B978-1-78242-118-4.00009-5. URL: http://dx.doi.org/10.1016/B978-1-78242-118-4.00009-5.

[11] Beznea E-F. Barcan M. Chirica I. "Numerical Vibro-Acoustic Analysis of a Ship Compartment Structure". In: *ITM Web of Conferences* 29 (2019). DOI: 10.1051/itmconf/20192902015. URL: https://www.itm-conferences.org/articles/itmconf/pdf/2019/06/itmconf_iccmae2018_02015.pdf.

[12] Ellson R. Hadimioglu B. Stearns R. "Moving Liquids with Sound: The Physics of Acoustic Droplet Ejection for Robust Laboratory Automation in Life Sci-

ences". In: *Journal of Laboratory Automation* 21 (1 2016), pp. 4–18. DOI: 10.1177/2211068215615096. URL: https://doi.org/10.1177/2211068215615096.

[13] Kunickaya L. Sharapov V. Sotula Z. "Piezoelectric electro-acoustic transducer". In: *The Journal of the Acoustical Society of America* 119 (5 2006). DOI: 10.1121/1.2203530.

[14] Charles L.A. Harris D.C. *Quantitative Chemical Analysis*. 10th ed. New York NY: W.H. Freeman and Company, 2020.

[15] Cortón E Mikkelsen S.R. *Bioanalytical Chemistry*. 2nd ed. Hoboken NJ: John Wiley Sons, Inc, 2016.

[16] Hage D.S. "Chromatography and electrophoresis". In: *Contemporary Practice in Clinical Chemistry* (2019), pp. 135–158. DOI: 10.1016/B978-0-12-815499-1.00008-9. URL: http://dx.doi.org/10.1016/B978-0-12-815499-1.00008-9.

[17] Dass N. Kumar A. Pathak P.P. "A Study of Speed of Sound in Water". In: *IOSR Journal of Applied Physics* 8 (4 2016), pp. 21–23. DOI: 10.9790/4861-0804022123.

[18] Jewett J.W. Jr. Serway R.A. *Physics for scientists and engineers with modern physics*. 9th ed. Boston MA: Cengage Learning, 2016.

[19] Destgeer G. Jung J.H. Park J. Ahmed H. Park K. Ahmad R. Sung H.J. "Acoustic impedance-based manipulation of elastic microspheres using travelling surface acoustic". In: *RSC Advances* (2017), pp. 22524–22530. DOI: 10.1039/c7ra01168g.

[20] Singh V.R. Lochab J. "Acoustic behavoir of plastics for medical applications". In: *Indian Journal of Pure Applied Physics* (2004), pp. 595–599.

A

Appendix 1

A.1 LC-MS method

A.1.1 Operating conditions

This section in Appendix 1 summarizes the operating conditions during the LC-MS method development and method use.

Table A.1: Mobile phase composition

Mobile phase composition	
A1	B1
1000 ml H_2O	1000 ml ACN (95%)
1 ml pH 3 acidic stock solution	1 ml pH 3 acidic stock solution

Table A.2: Acidic stock solution composition

pH 3 acidic stock solution
126.3 g H_2O
151.8 g formic acid
21.8 g ammonium hydroxide solution (NH_3 25 - 30 %)

Table A.3: Weak wash composition

Weak wash	
H_2O	900 ml
MeOH	100 ml

Table A.4: Strong wash composition

Strong wash	
H_2O	250 ml
MeOH	250 ml
ACN	250 ml
isopropanol	250 ml
formic acid	5 ml

Table A.5: Mobile phase gradient

Time (min)	Flow (ml/min)	% A1	% B1
initial	1	90.0	10.0
0.20	1	90.0	10.0
1.70	1	1.0	99.0
1.80	1	1.0	99.0
1.81	1	90.0	10.0
2.00	1	90.0	10.0

Table A.6: Sample manager- and column temperatures

Temperatures	
Sample manager	Column
20 °C	60 °C

Table A.7: Injection settings

Autosampler settings	
Split/splitless	Split
Loop volume	2 μl
Syringe volume	10 μl
Syringe drawrate	25 μl/min

A.1.2 Concentration and injection volume tests

The following section in Appendix 1 summarizes the results from the method development, where seven different injection volumes are tested for four different concentrations. The tables include the integrated peak area for compound AZ1217530 for each injection volume and concentration.

Table A.8: Integrated peak area for injection volumes between 0.4 - 1.0 μl for a 10 mM DMSO solution of compound AZ1217530

10 mM	
Injection volume (μl)	Peak area (a.u.)
0.4	874 683
0.5	1 458 835
0.6	1 668 925
0.7	1 825 125
0.8	2 050 354
0.9	2 186 919
1.0	2 363 286

Table A.9: Integrated peak area for injection volumes between 0.4 - 1.0 μl for a 5 mM DMSO solution of compound AZ1217530

5 mM	
Injection volume (μl)	Peak area (a.u.)
0.4	581 631
0.5	671 050
0.6	801 953
0.7	935 444
0.8	1 071 700
0.9	1 210 836
1.0	1 305 580

Table A.10: Integrated peak area for injection volumes between 0.4 - 1.0 μl for a 2.5 mM DMSO solution of compound AZ1217530

2.5 mM	
Injection volume (μl)	Peak area (a.u.)
0.4	136 742
0.5	209 161
0.6	268 718
0.7	325 553
0.8	376 656
0.9	426 801
1.0	459 104

Table A.11: Integrated peak area for injection volumes between 0.4 - 1.0 μl for a 1.25 mM DMSO solution of compound AZ1217530

1.25 mM	
Injection volume (μl)	Peak area (a.u.)
0.4	49 533
0.5	75 032
0.6	101 770
0.7	122 578
0.8	143 771
0.9	172 215
1.0	203 869

A.1.3 Method development graphs

The following section displays the linear relationship between the integrated peak area and increasing injection volumes and concentrations.

A.1.3.1 Relationship between integrated peak area and increasing injection volume

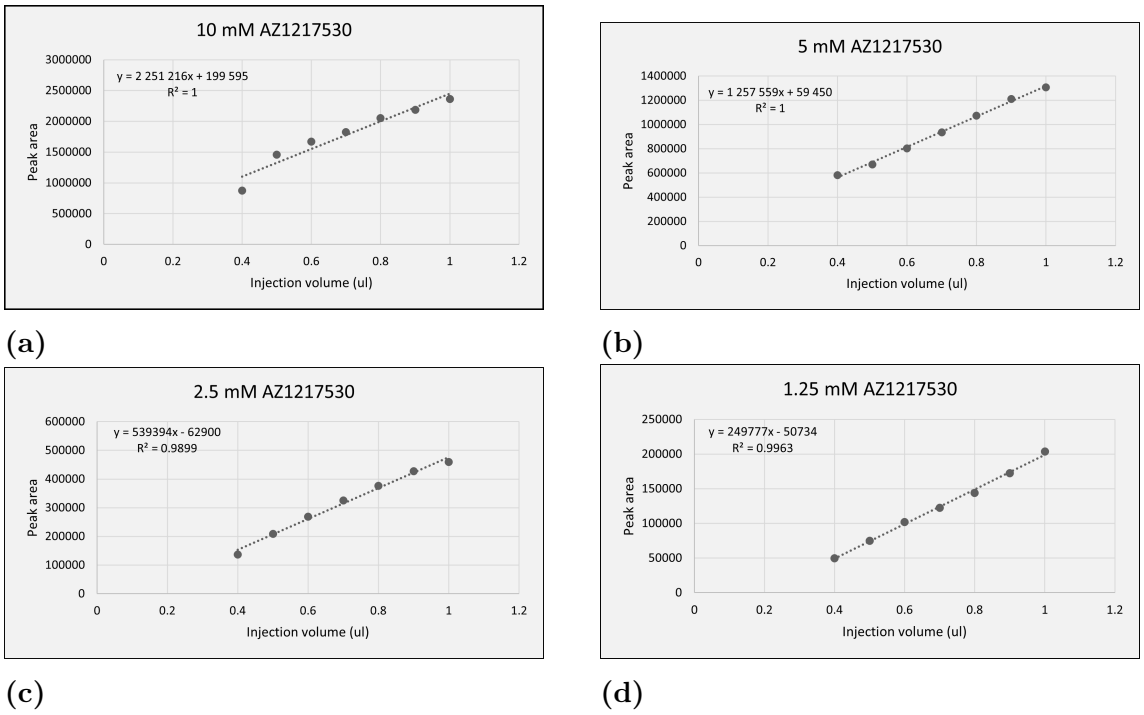

Figure A.1: Four graphs displaying the linear relationship between the integrated peak area and increasing injection volume, for seven different injection volumes between 0.4 - 1.0 μl at four different concentrations of AZ1217530 dissolved in DMSO.

A.1.3.2 Relationship between integrated peak area and increasing concentration

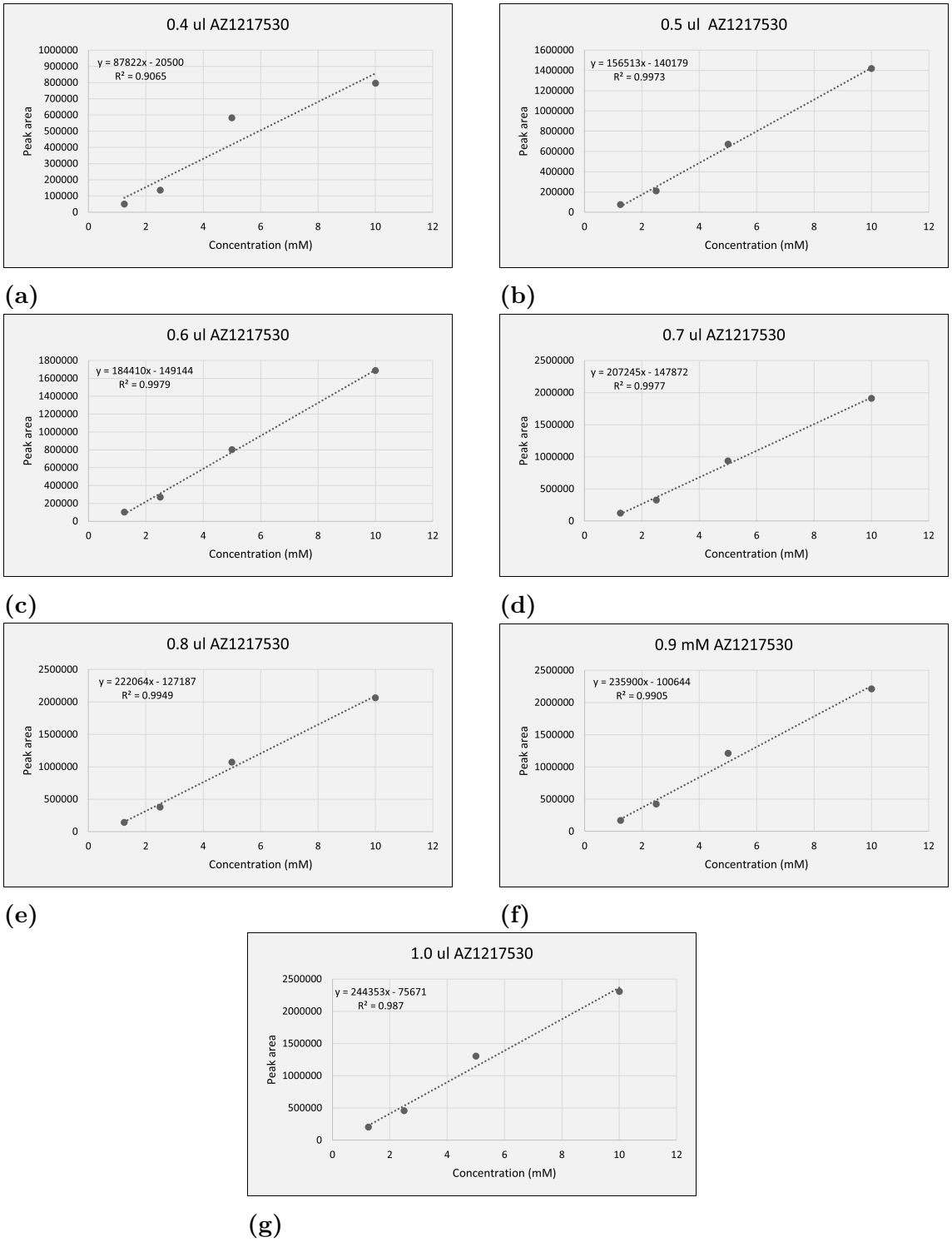

Figure A.2: Seven graphs displaying the linear relationship between the integrated peak area of compound AZ1217530 and increasing concentrations between 1.25 - 10 mM, for seven different injection volumes between 0.4 - 1.0 μl.

B

Appendix 2

B.1 Volume measurements

The following section summarizes the results from the initial and repeated volume measurements on the acquired set of samples. Displayed in Table B.1 on the next page are the total number of successful measurements for each of the 50 compounds. Highlighted in red are the compounds that showed different results in the repeated experiment compared to the initial 50 measurements.

Table B.1: List of compounds in acquired set, together with the number of successful initial volume measurements and number of successful repeated volume measurement. Compounds that deviate from consistent results are highlighted in red.

Compound ID	Successful volume measurements (out of 50)	Successful volume measurements in repeated experiment (out of 1)
AZ14243461	50	1
AZ14250073	50	1
AZ14252290	50	1
AZ14260181	50	1
AZ14274477	50	1
AZ14265490	49	1
AZ14336781	50	1
AZ10466261	50	1
AZ11351386	50	1
AZ14245813	49	1
AZ14250186	50	1
AZ14254516	50	1
AZ14264547	50	1
AZ14276920	50	1
AZ14333177	50	1
AZ14336782	50	1
AZ10033450	50	1
AZ14177187	50	1
AZ14247552	50	1
AZ14233546	50	1
AZ14254949	50	1
AZ14264750	50	0
AZ14278316	50	0
AZ14333194	50	1
AZ14264652	50	1
AZ10528650	50	1
AZ14260218	50	1
AZ14247555	50	1
AZ14250659	50	1
AZ14255240	50	1
AZ14264751	50	0
AZ14278325	50	1
AZ14340727	50	1
AZ10534736	50	1
AZ14254260	50	1
AZ14248166	50	1
AZ14253109	0	1
AZ14192861	0	0
AZ14267257	0	1
AZ14278321	50	1
AZ14340540	0	1
AZ10537633	50	1
AZ14262702	50	1
AZ14248428	50	1
AZ14251990	50	1
AZ14256291	50	0
AZ14268657	50	0
AZ14279000	50	1
AZ14192861	50	0
AZ12054477	50	1
AZ14241926	50	0
AZ14248562	50	1
AZ14252110	50	1
AZ14258874	50	0
AZ14273466	0	1
AZ14281641	0	1
AZ13849461	50	1
AZ10829511	50	1
AZ14241896	48	1
AZ14249811	50	0
AZ14335208	50	1
AZ14259602	50	1
AZ14273546	50	1
AZ14283201	0	1

C

Appendix 3

C.1 Absorption results

The following section summarizes the results from the LC-MS method for all 50 compounds. Displayed in Table C.1 on the next page, are all the integrated peak areas, together with the pak area ratio, retention time and molar mass for each compound.

Table C.1: List of all substances in the acquired set, together with their respective molar mass, retention time in selected LC method, peak areas and peak area ratios.

Sample	Compound ID	Molar mass	Retention time	Non diluted peak area	Diluted peak area	Peak area ratio
1	AZ14243461	465.50	0.8725	67 818.37	217 575.41	3.21
2	AZ14250073	500.60	1.0609	27 247.66	304 997.59	11.19
3	AZ14252290	471.60	0.6988	72 082.59	389 347.59	5.40
4	AZ14260181	439.40	0.9784	134 811.50	191 467.06	1.42
5	AZ14265490	552.10	0.5213	183 902.84	106 771.10	0.58
6	AZ10466261	336.30	0.6108	444 545.13	369 749.16	0.83
7	AZ14245813	489.50	0.8225	85 994.67	217 839.97	2.53
8	AZ14250186	475.50	0.6725	99 923.24	222 898.31	2.23
9	AZ14254516	288.30	0.5479	132 417.81	51 740.46	0.39
10	AZ14264547	457.50	0.6354	1 935 249.75	218 559.17	0.11
11	AZ14276920	513.55	0.8867	34 040.43	229 816.73	6.75
12	AZ14333177	400.44	1.0113	13 442.23	58 661.67	4.36
13	AZ10033450	272.30	0.8271	9 481.40	331 696.47	34.98
14	AZ14177187	477.00	1.525	14 712.11	18 354.30	1.25
15	AZ14247552	475.50	0.6204	142 892.67	1 006 903.44	7.05
16	AZ14233546	447.50	1.005	106 352.63	1 099 144.75	10.33
17	AZ14264750	475.50	0.5925	166 727.88	312 269.66	1.87
18	AZ14278316	513.55	0.9075	71 547.64	240 936.45	3.37
19	AZ14260218	313.30	0.3358	38 953.25	184 528.34	4.74
20	AZ14250659	531.60	0.7263	241 454.67	251 586.06	1.04
21	AZ14255240	404.40	0.6146	384 109.81	236 076.80	0.61
22	AZ14264751	468.50	0.8379	73 704.75	149 388.47	2.03
23	AZ14278325	513.55	1.0367	31 560.31	332 164.09	10.52
24	AZ14340727	410.51	0.1917	514 114.06	61 157.65	0.12
25	AZ14254260	?	0.4658	4 724 552.00	?	?
26	AZ14253109	446.50	0.7038	325 885.66	172 612.41	0.53
27	AZ14192861	461.50	0.8838	44 081.60	258 898.33	5.87
28	AZ14278321	512.56	0.7438	321 380.47	200 902.42	0.63
29	AZ14340540	581.02	1.0884	4 811.81	212 679.64	44.20
30	AZ14262702	377.30	0.8438	20 243.79	2 822 213.00	139.41
31	AZ14248428	397.50	0.7213	9 447.48	341 997.44	36.20
32	AZ14251990	305.40	0.7517	28 006.37	157 208.02	5.61
33	AZ14256291	461.50	0.8146	275 952.34	511 498.22	1.85
34	AZ14268657	494.50	1.0146	142 223.20	529 973.69	3.73
35	AZ14279000	801.94	0.6063	22 351.44	230 281.34	10.30
36	AZ14192861	461.50	0.8238	198 453.28	243 114.11	1.23
37	AZ12054477	357.80	1.6696	13 596.57	106 228.54	7.81
38	AZ14241926	420.50	0.9604	40 512.18	700 995.19	17.30
39	AZ14248562	521.60	0.8004	147 256.64	102 192.74	0.69
40	AZ14252110	477.50	0.7171	239 554.41	89 014.52	0.37
41	AZ14258874	458.50	0.9688	13 1303.80	340 469.72	2.59
42	AZ14273466	489.57	0.9384	577 736.63	465 774.06	0.81
43	AZ14281641	518.57	0.7917	19 753.47	47 160.64	2.39
44	AZ10829511	287.30	0.8075	531 487.81	56 526.63	0.11
45	AZ14241896	461.50	0.9246	67 834.49	71 378.37	1.05
46	AZ14249811	518.70	0.5096	394 457.38	294 289.34	0.75
47	AZ14335208	400.48	0.6933	545 433.13	66 090.87	0.12
48	AZ14259602	458.50	0.9709	192 133.34	203 809.45	1.06
49	AZ14273546	777.89	0.9304	11 668.78	44 614.59	3.82
50	AZ14283201	582.45	0.7208	317 565.56	401 099.53	1.26

D

Appendix 4

D.1 Grid survey results

The following section summarizes the results from the grid survey on the acoustic tubes containing PMMA microspheres. Tables D.1, D.2, D.3, D.4 and D.5 represent the five different sphere sizes, and display the number of interference points where a 0-height measurement is obtained and the fraction of total measurement points that is represented by that number. The tables also display whether the volume could be determined or if the tubes where left immeasurable.

Table D.1: Summary of grid survey for spheres of 29.98 μm radius with the number of interference points corresponding to the fraction of covered acoustic tube bottom and the possibility to measure the volume of the tube content, for the 8 different concentrations.

29.98 μm			
Dilution	Interference points	Fraction of interfered area	Measurable
1:1	896	53%	Yes
1:2	974	58%	No
1:4	778	46%	Yes
1:8	857	51%	No
1:16	816	49%	Yes
1:32	809	48%	Yes
1:64	732	43%	Yes
1:128	786	47%	Yes

Table D.2: Summary of grid survey for spheres of 60.1 μm radius with the number of interference points corresponding to the fraction of covered acoustic tube bottom and the possibility to measure the volume of the tube content, for the 8 different concentrations.

60.1 μm			
Dilution	Interference points	Fraction of interfered area	Measurable
1:1	1443	86%	No
1:2	1153	69%	No
1:4	1188	71%	No
1:8	1017	61%	Yes
1:16	784	47%	Yes
1:32	807	48%	Yes
1:64	708	42%	Yes
1:128	789	47%	Yes

Table D.3: Summary of grid survey for spheres of 101 μm radius with the number of interference points corresponding to the fraction of covered acoustic tube bottom and the possibility to measure the volume of the tube content, for the 8 different concentrations.

101 μm			
Dilution	Interference points	Fraction of interfered area	Measurable
1:1	1248	74%	No
1:2	1198	71%	No
1:4	1316	78%	No
1:8	943	56%	Yes
1:16	801	48%	Yes
1:32	832	49%	Yes
1:64	767	46%	Yes
1:128	746	44%	Yes

Table D.4: Summary of grid survey for spheres of 127 μm radius with the number of interference points corresponding to the fraction of covered acoustic tube bottom and the possibility to measure the volume of the tube content, for the 8 different concentrations.

127 μm			
Dilution	Interference points	Fraction of interfered area	Measurable
1:1	839	50%	No
1:2	939	56%	No
1:4	805	48%	No
1:8	791	47%	Yes
1:16	761	45%	Yes
1:32	753	45%	Yes
1:64	787	47%	Yes
1:128	753	45%	Yes

Table D.5: Summary of grid survey for spheres of 148 μm radius with the number of interference points corresponding to the fraction of covered acoustic tube bottom and the possibility to measure the volume of the tube content, for the 8 different concentrations.

148 μm			
Dilution	Interference points	Fraction of interfered area	Measurable
1:1	787	47%	Yes
1:2	849	51%	No
1:4	827	49%	Yes
1:8	809	48%	Yes
1:16	781	46%	Yes
1:32	769	46%	Yes
1:64	773	46%	Yes
1:128	785	47%	Yes

D.2 Grid survey maps

The figures on the following pages in this section display the results from the grid survey depicted in 2D and 3D graphs. The blue measurement points represent the 0-height measurements and the yellow measurement points represent the maximum height measurements.

D.2.1 29.98 μm

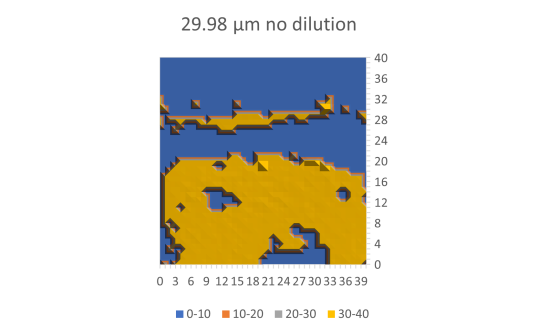

(a)

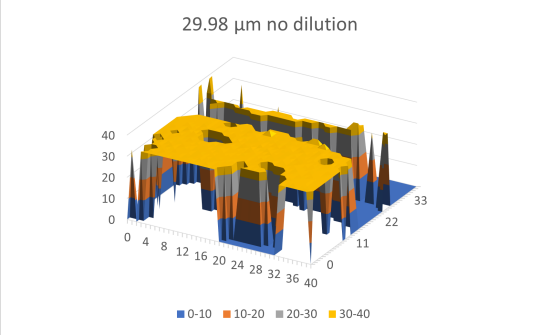

(b)

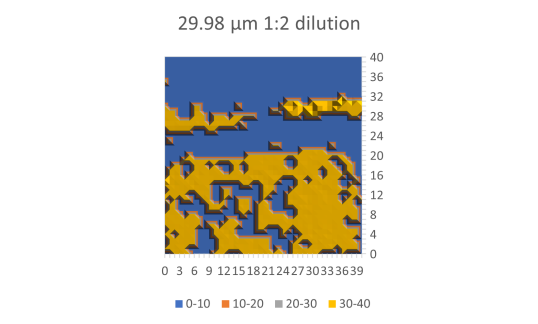

(c)

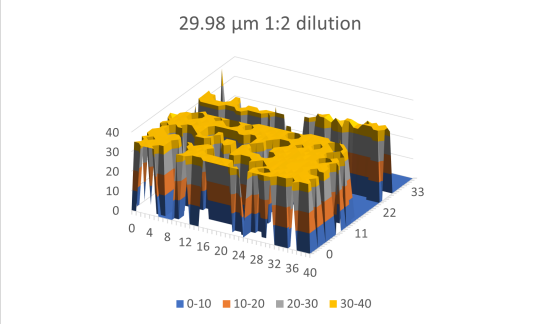

(d)

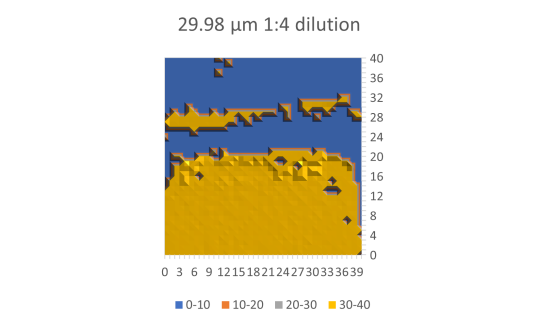

(e)

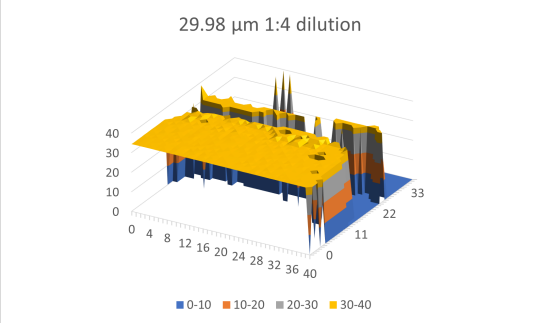

(f)

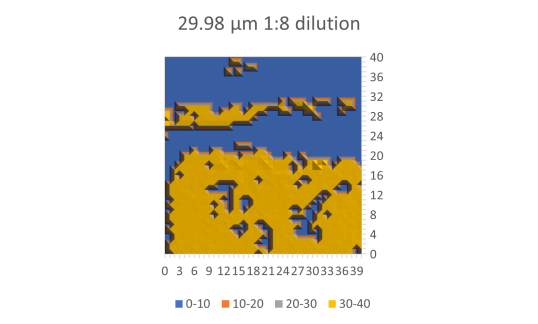

(g)

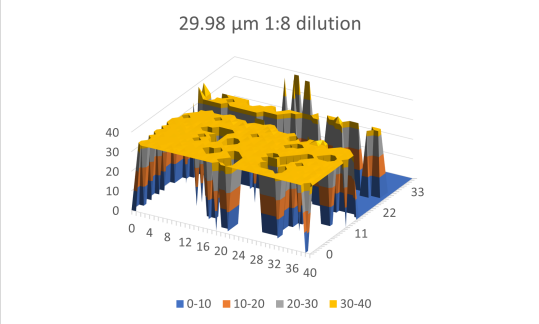

(h)

Figure D.1: 2D and 3D illustrations of the recorded coverage and measured fluid height during grid survey for spheres of 29.98 μm radius. *cont.*

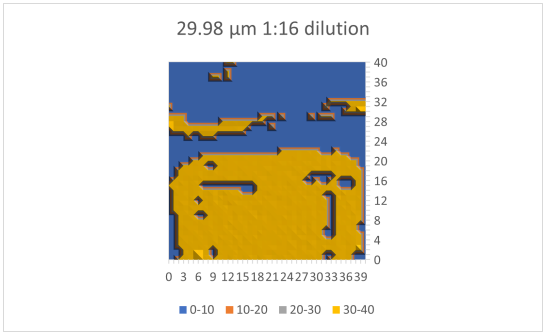

(i)

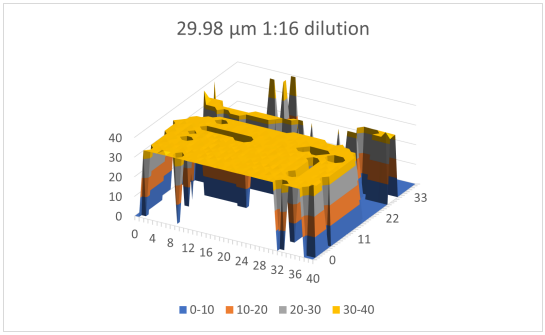

(j)

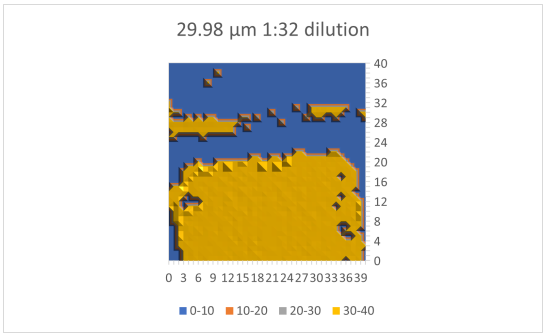

(k)

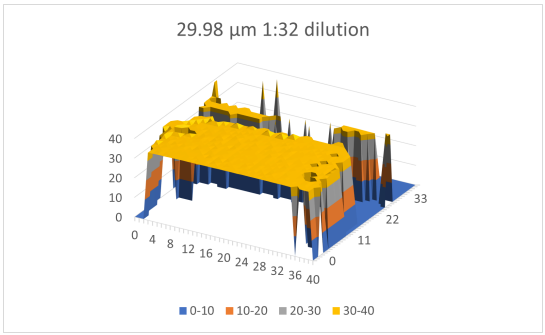

(l)

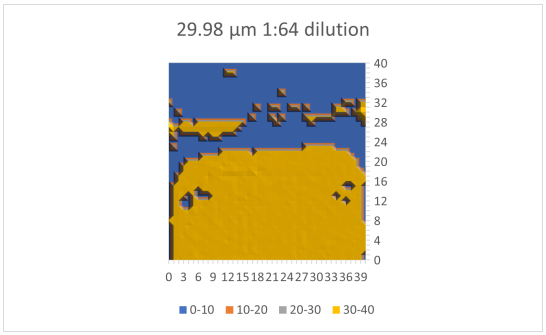

(m)

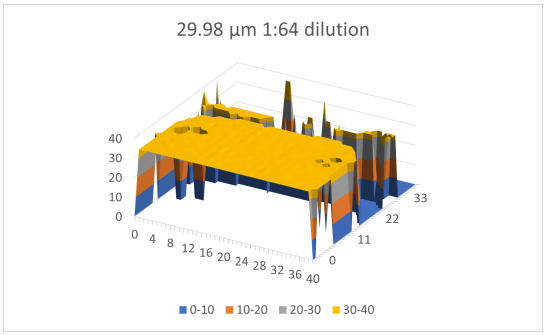

(n)

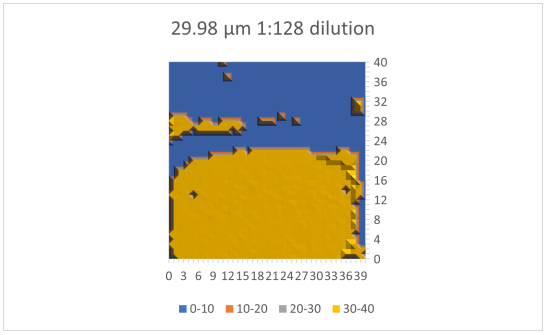

(o)

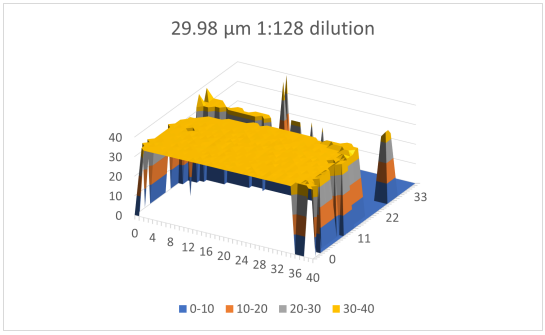

(p)

Figure D.1: 2D and 3D illustrations of the recorded coverage and measured fluid height during grid survey for spheres of 29.98 μm radius.

D.2.2 60.1 μm

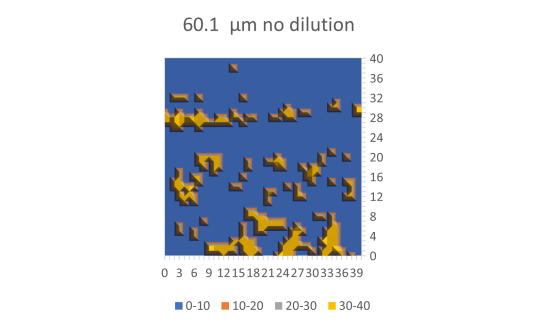

(a)

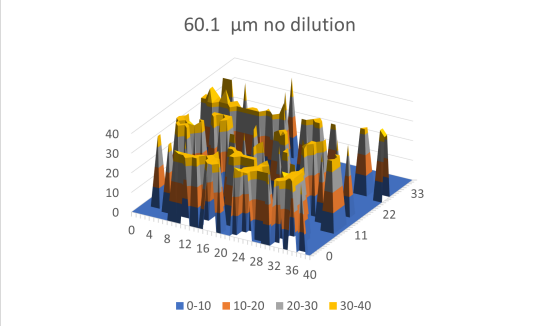

(b)

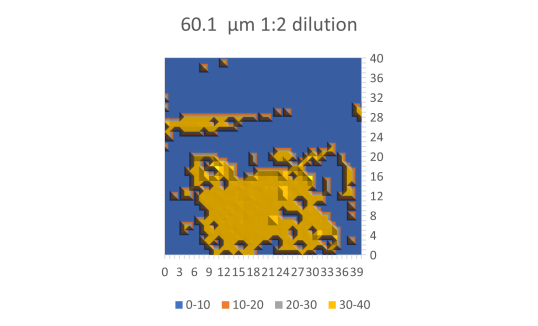

(c)

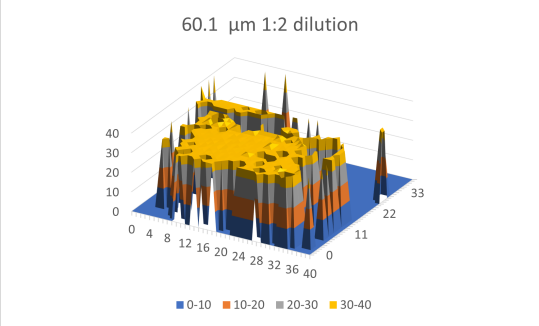

(d)

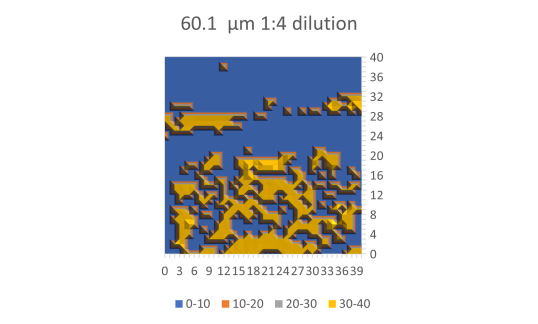

(e)

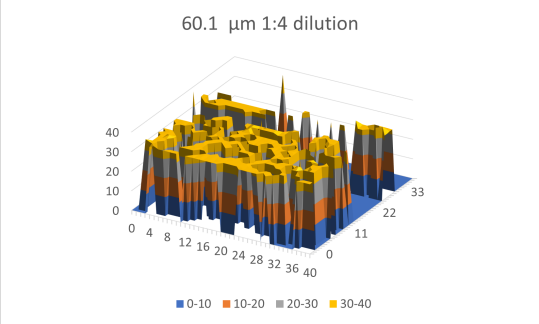

(f)

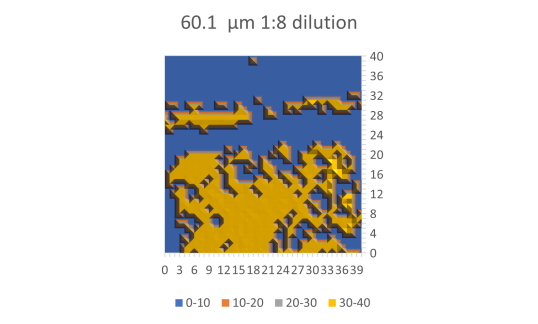

(g)

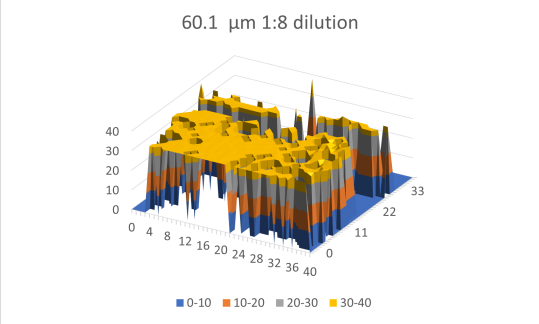

(h)

Figure D.2: 2D and 3D illustrations of the recorded coverage and measured fluid height during grid survey for spheres of 60.1 μm radius. *cont.*

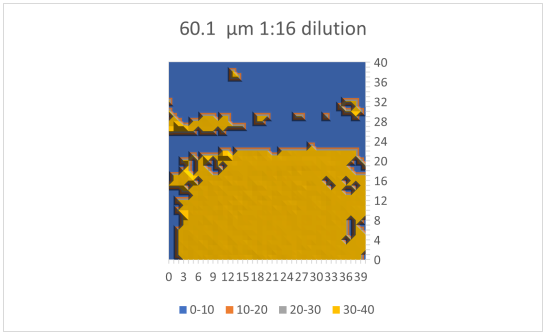

(i)

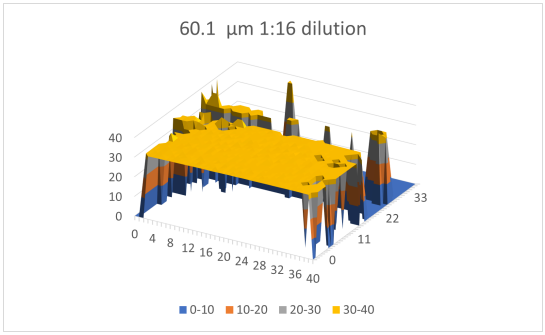

(j)

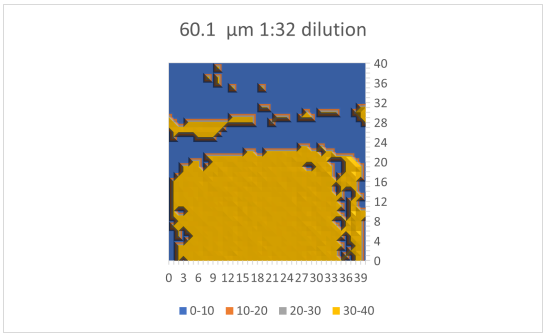

(k)

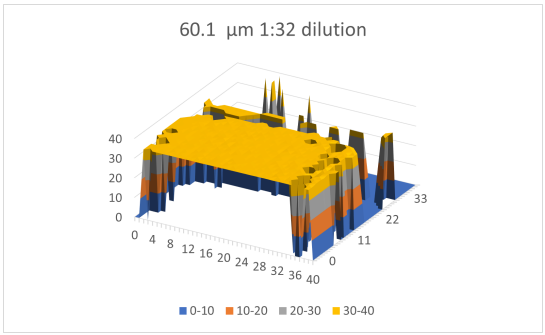

(l)

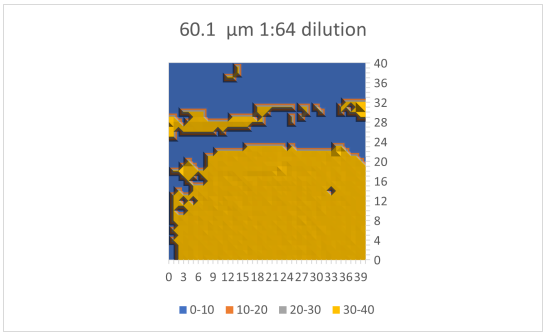

(m)

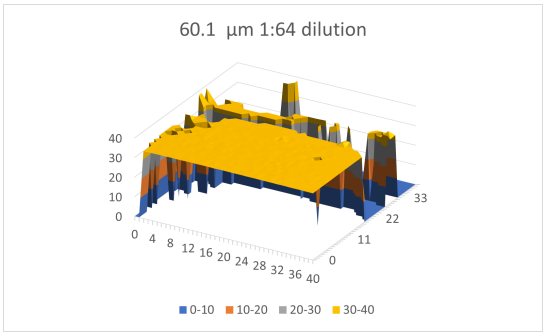

(n)

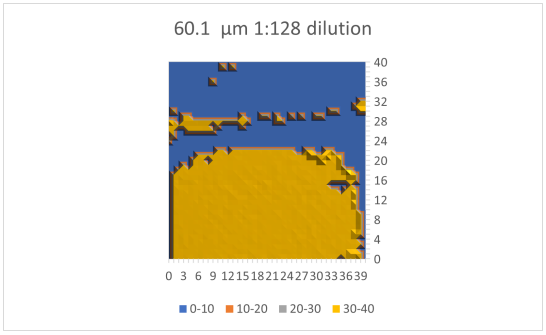

(o)

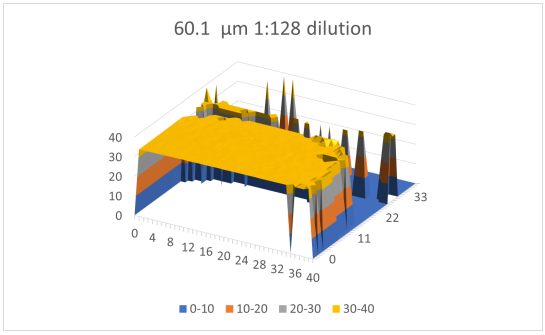

(p)

Figure D.2: 2D and 3D illustrations of the recorded coverage and measured fluid height during grid survey for spheres of 60.1 μm radius.

D.2.3 101 μm

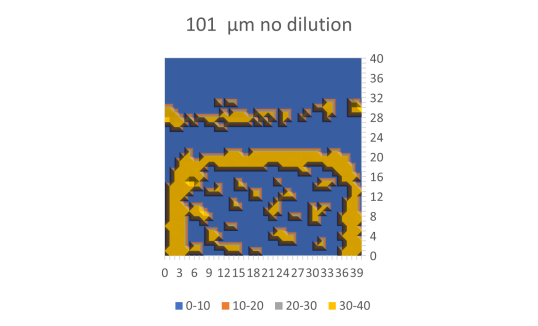

(a)

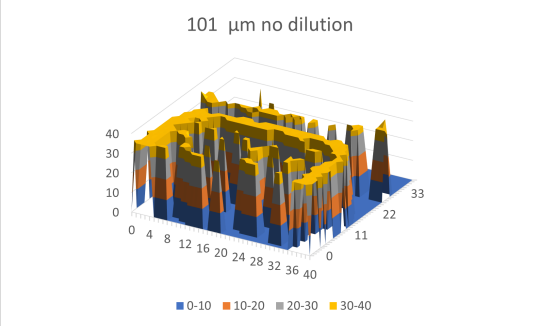

(b)

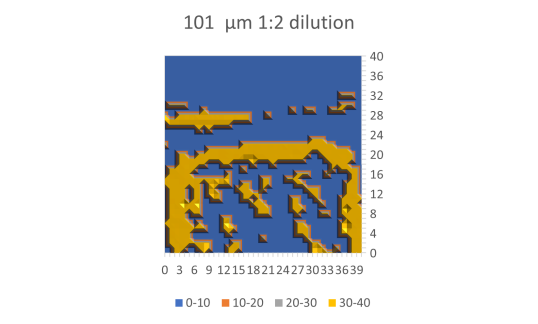

(c)

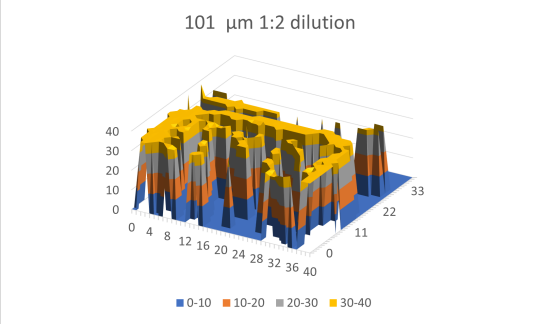

(d)

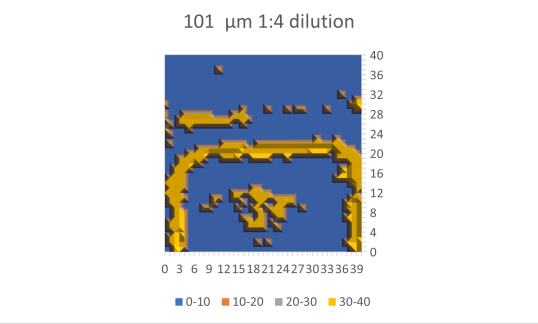

(e)

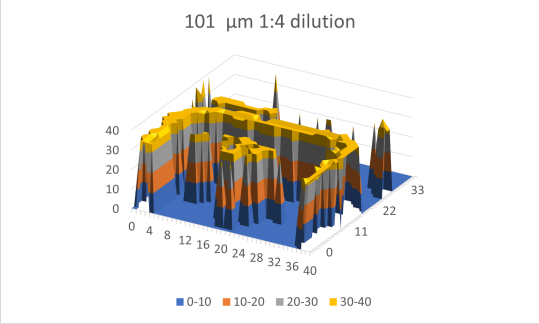

(f)

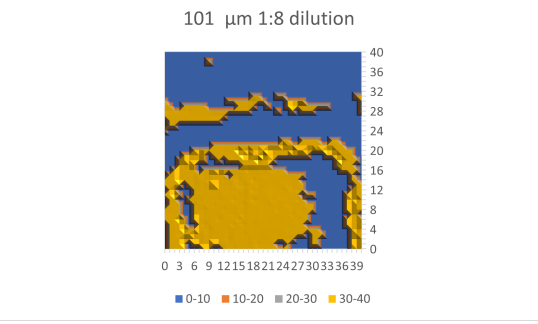

(g)

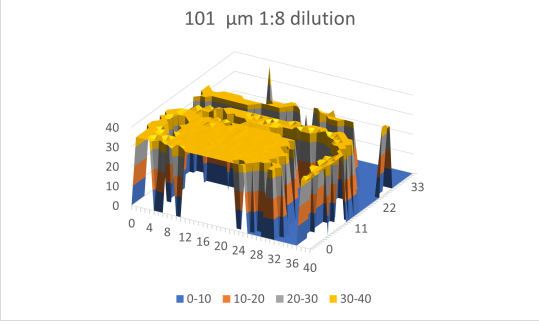

(h)

Figure D.3: 2D and 3D illustrations of the recorded coverage and measured fluid height during grid survey for spheres of 101 μm radius. *cont.*

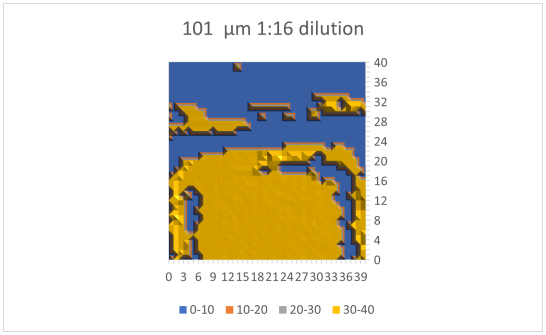

(i)

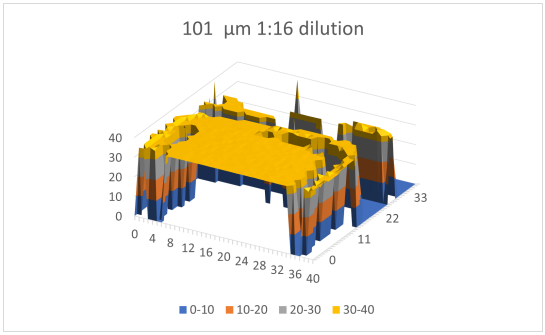

(j)

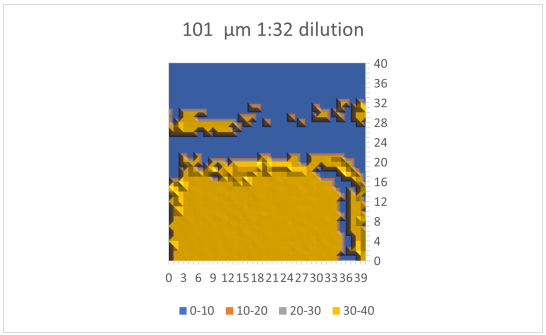

(k)

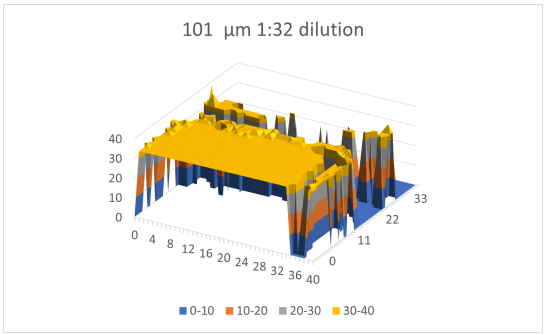

(l)

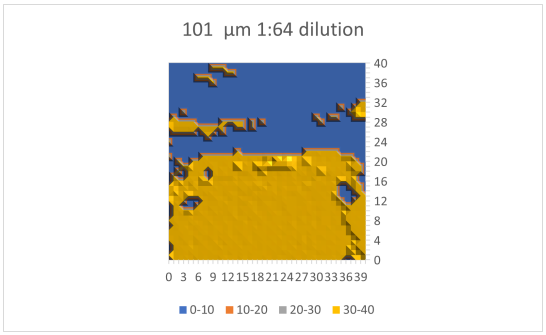

(m)

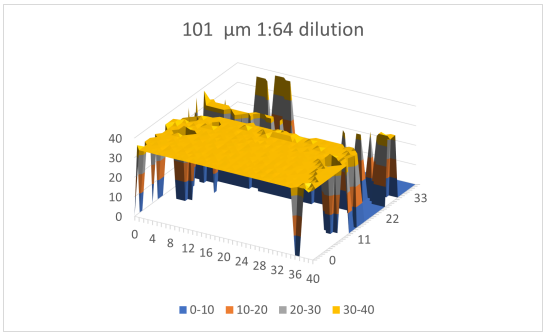

(n)

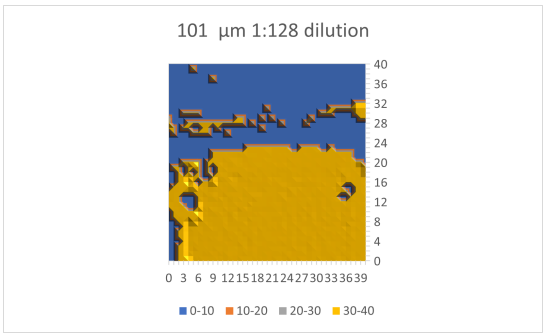

(o)

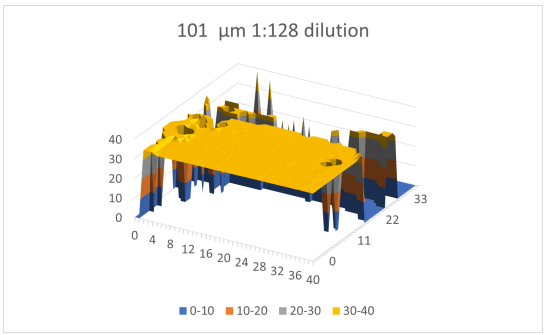

(p)

Figure D.3: 2D and 3D illustrations of the recorded coverage and measured fluid height during grid survey for spheres of 101 μm radius.

D.2.4 127 μm

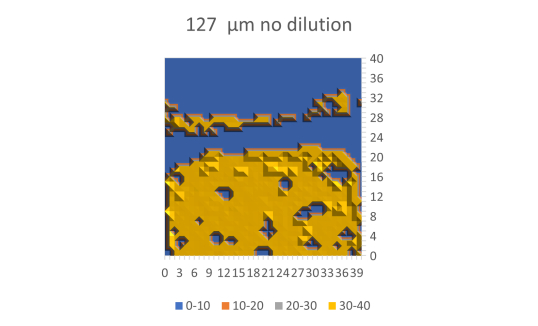

(a)

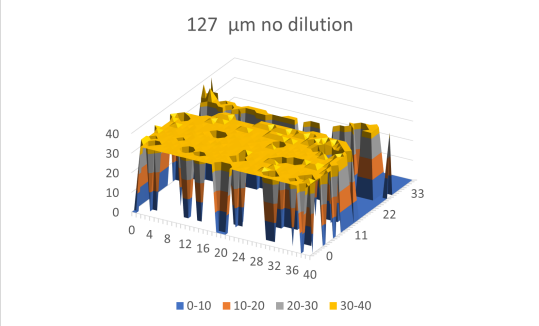

(b)

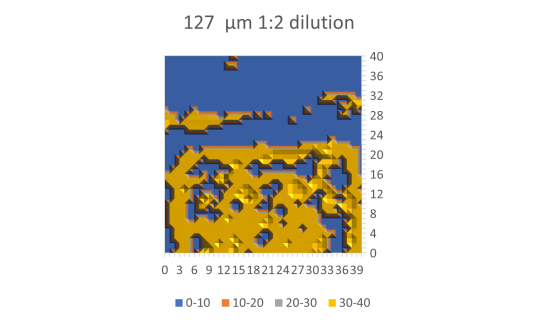

(c)

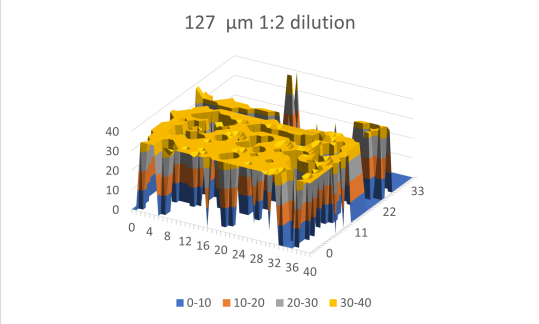

(d)

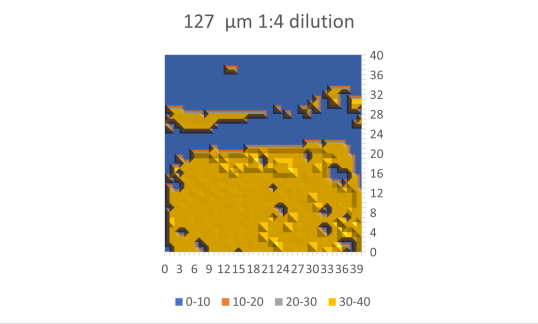

(e)

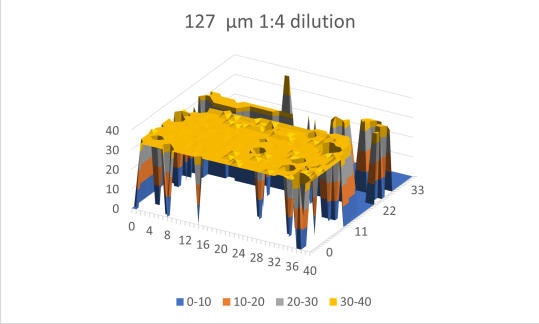

(f)

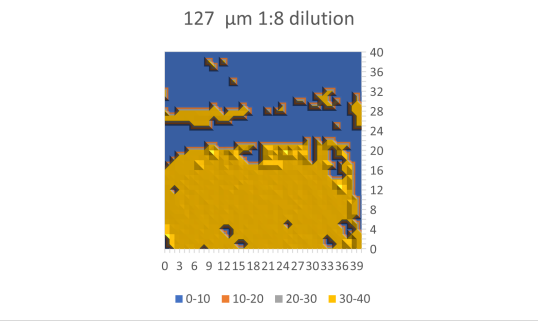

(g)

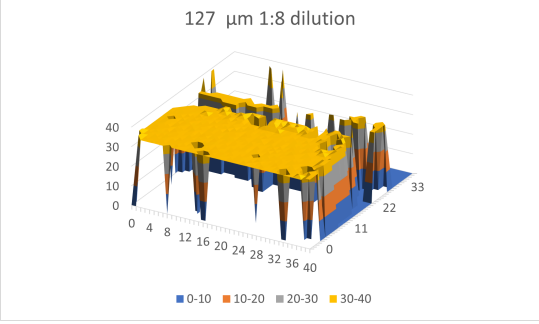

(h)

Figure D.4: 2D and 3D illustrations of the recorded coverage and measured fluid height during grid survey for spheres of 127 μm radius. *cont.*

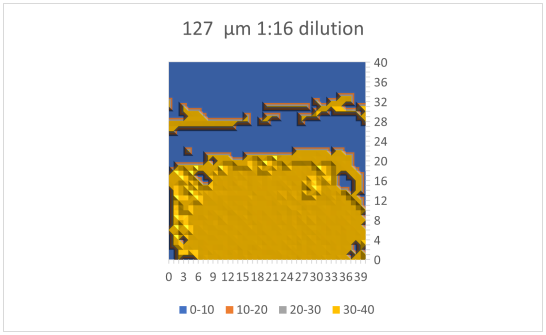

(i)

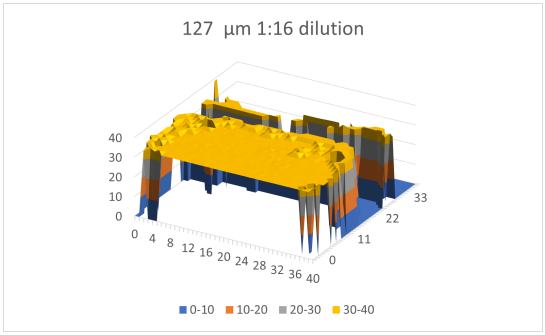

(j)

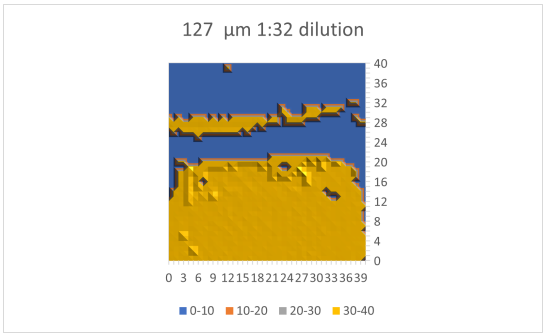

(k)

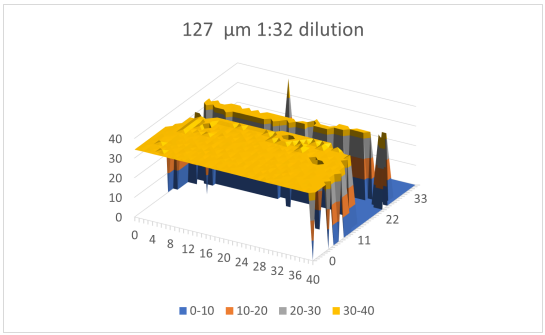

(l)

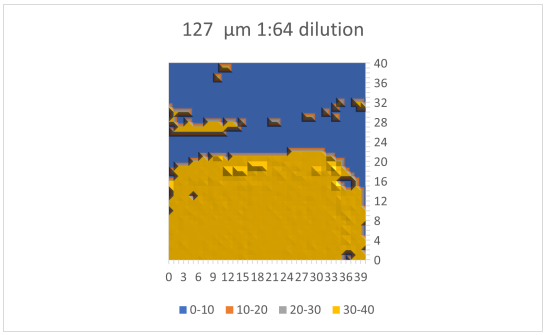

(m)

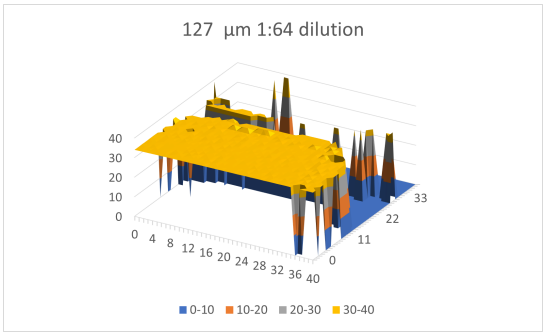

(n)

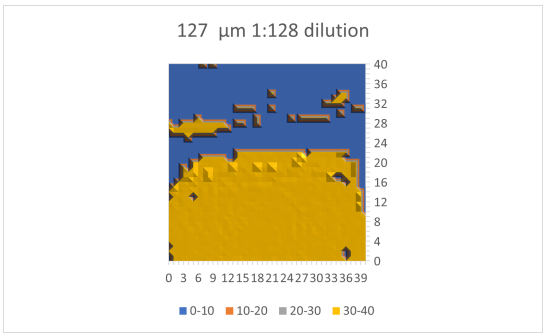

(o)

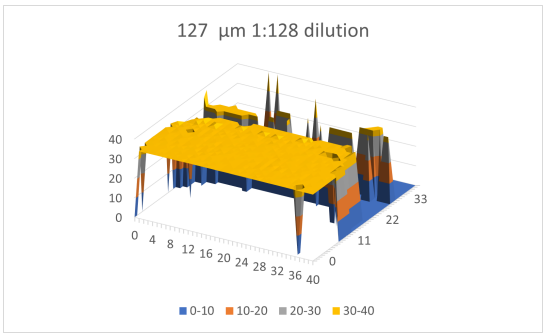

(p)

Figure D.4: 2D and 3D illustrations of the recorded coverage and measured fluid height during grid survey for spheres of 127 μm radius.

D.2.5 148 μm

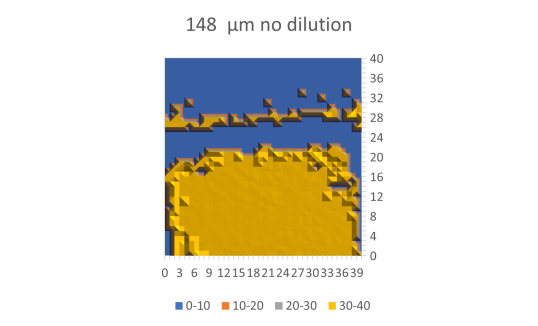

(a)

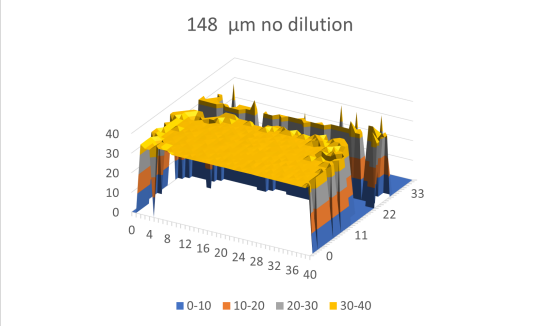

(b)

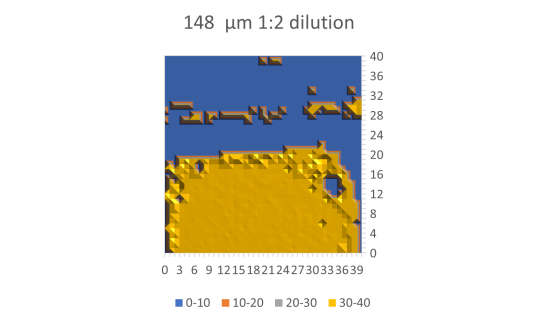

(c)

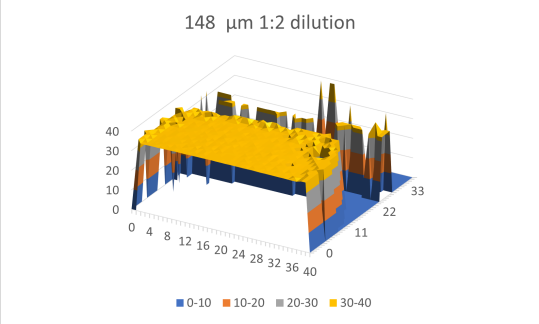

(d)

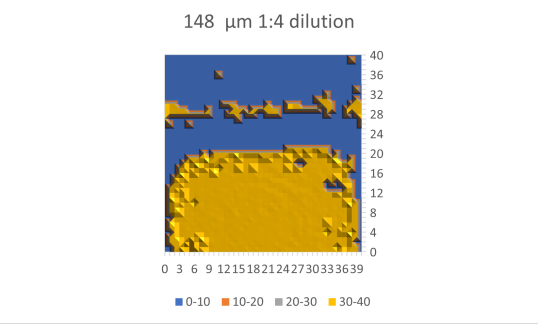

(e)

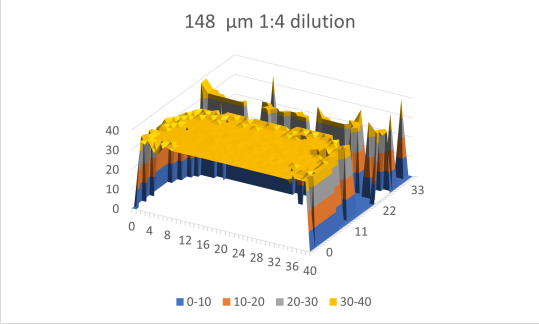

(f)

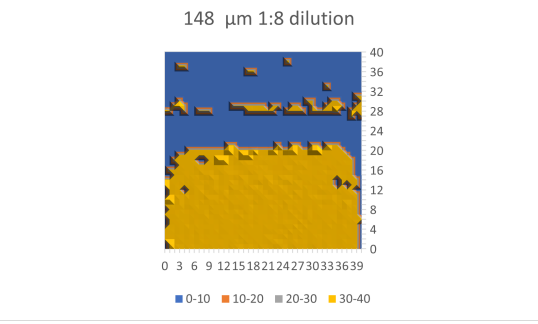

(g)

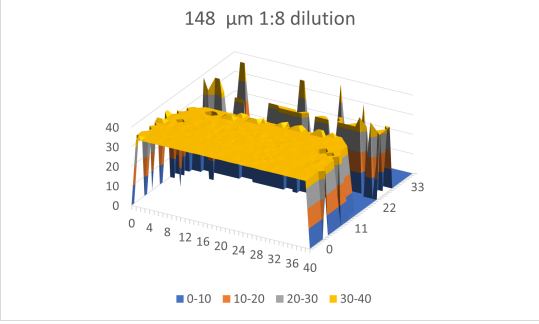

(h)

Figure D.5: 2D and 3D illustrations of the recorded coverage and measured fluid height during grid survey for spheres of 148 μm radius. *cont.*

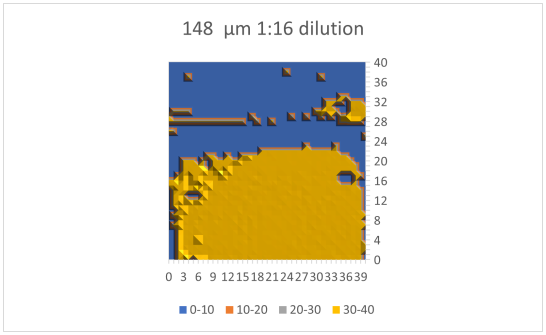

(i)

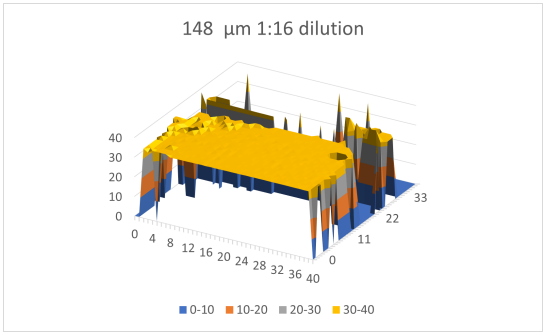

(j)

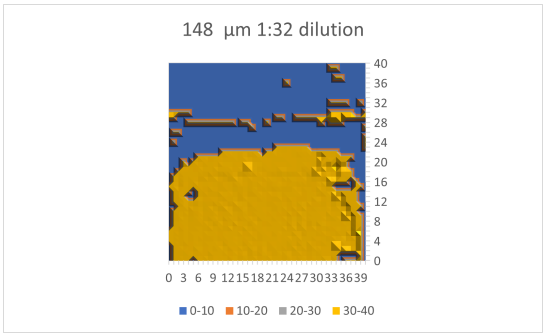

(k)

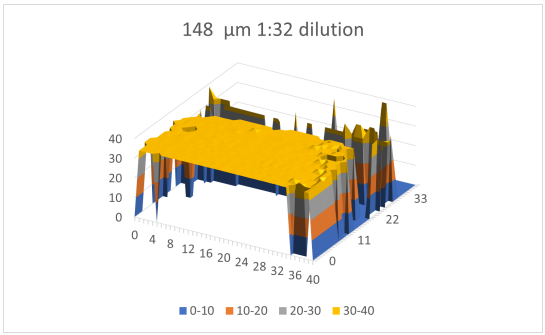

(l)

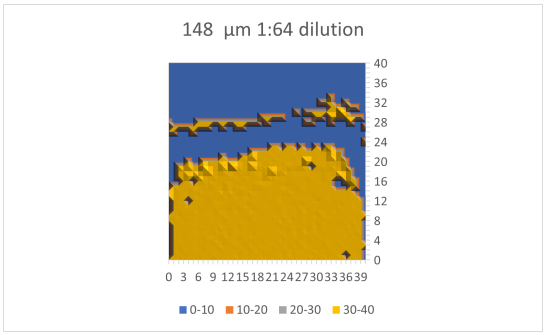

(m)

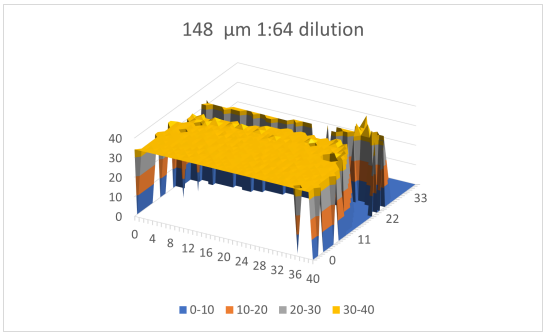

(n)

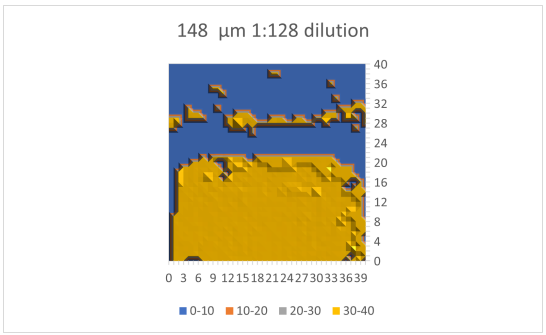

(o)

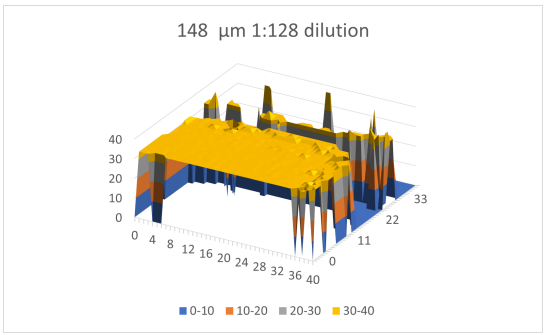

(p)

Figure D.5: 2D and 3D illustrations of the recorded coverage and measured fluid height during grid survey for spheres of 148 μm radius.

DEPARTMENT OF SOME SUBJECT OR TECHNOLOGY
CHALMERS UNIVERSITY OF TECHNOLOGY
Gothenburg, Sweden
www.chalmers.se

CHALMERS
UNIVERSITY OF TECHNOLOGY